Norwegian University of Life Sciences
Faculty of Environmental Science and Technology
Department of Mathematical Sciences and Technology

Master Thesis 2015
30 credits

Analysis of Grid-Connected Wind Farm Combined With Hydrogen Production

Lotte Løland

Preface

The present work was carried out at the Department of Mathematical Sciences and Technology at the Norwegian University of Life Science (NMBU) from January to May 2015. My supervisor was Professor Tor Anders Nygaard in Mechanics and Process Technology at NMBU. My co-advisor has been Dr. Steffen Møller-Holst, vice president marketing at SINTEF.

Acknowledgements

I want to thank my supervisor Prof. Tor Anders Nygaard for guidance and advising throughout the work of the thesis. He has helped me in every aspect. His broad experience with analyzing data and developing simulation codes has been particularly valuable. I also want to thank my co-advisor Dr. Steffen Møller-Holst for his contributions. He has helped me understanding the characteristics of the hydrogen market and been an important reference for quality assurance of assumptions and results.

A huge thanks goes to Kjeller Vindteknikk and Thomas Mo Willig, for running a Weather Research and Forecast model for the purpose of this thesis. I also want to thank Tore Martinsen and Tom Wilhelm Reisænen in Varanger KraftVind for sharing production data from Raggovidda wind farm.

Bjørn Simonsen, NEL Hydrogen, and Øivind Korneliussen, Varanger KraftNett have been very helpful by sharing their knowledge and useful data. A thanks also goes to Maria Spångberg for giving me access to the Nord Pool Spot database.

Ås, 13th of May, 2015

_____

Lotte Løland

Abstract

Raggovidda wind farm is assumed expanded from 45 MW to 200 MW, and hydrogen is assumed produced from excess wind power. The grid restriction is 50 MW, and whenever the wind power exceeds 50 MW, hydrogen is produced.

Based on a Weather Research and Forecast model run by Kjeller Vindteknikk, as well as wind- and production data from Raggovidda wind farm, a time-series of 20 years of wind power with an hourly resolution is developed. With this as an input, hydrogen production is simulated with the use of Python. Alkaline atmospheric electrolysers of 2.3 MW are considered. Liquid storage and delivery is considered the best solution. The storage is assumed emptied once a week, and hydrogen is delivered by two liquid carrier ships in shuttle with a range of 2,000-2,500 nautic miles. Electrolyser and storage capacity are design variables. Liquefaction capacity follows from the electrolysis maximum output, and the ship size required follows from the storage capacity.

By minimizing production costs, the optimal dimensions of the plant are found. The optimal electrolysis capacity ranges from 103.5 – 151.8 MW and the optimal weekly storage ranges from 300 – 400 tons of hydrogen, provided a 5 % result cost interval. This requires a liquefaction capacity of 49 – 58 tons/day, and a carrier ship size of 4,240 - 5,650 m^3. The minimum production cost is calculated to 4.23 – 4.34 EUR/kg. With a charge of about 10 EUR/kg hydrogen at refuelling stations, a revenue of more than 5 EUR/kg may be achievable, provided no VAT or taxes are added.

Contents

ABBREVIATIONS ..... **VII**

LIST OF FIGURES ..... **IX**

LIST OF TABLES ..... **XI**

1 INTRODUCTION **1**

1.1 WIND POWER IN NORWAY 2

1.2 THE ENERGY SITUATION IN BERLEVÅG 3

1.3 SCOPE OF THE THESIS 5

2 BACKGROUND **7**

2.1 WIND POWER 7

2.2 HYDROGEN 10

2.2.1 Fundamentals *10*

2.2.2 Hydrogen usage *11*

2.2.3 The hydrogen market *12*

2.3 THE PRODUCTION PROCESS 13

2.3.1 Water Electrolysis *13*

2.3.2 Compression *16*

2.3.3 Liquefaction *17*

2.3.4 Storage *20*

2.3.5 Delivery *24*

2.4 ECONOMICS 27

3 METHODS **29**

3.1 PLANT SPECIFICATIONS 29

3.1.1 Wind farm *29*

3.1.2 Electrolyser *30*

3.1.3 Liquefier *31*

3.1.4 Storage *31*

3.1.5 Delivery *31*

3.2 COST CALCULATIONS 32

3.2.1 Electricity income *33*

3.3 DEVELOPMENT OF A TIME-SERIES OF POWER 34

3.3.1 Wind series *35*

3.3.2 Power series *37*

3.4 PLANT SIMULATIONS 39

4 RESULTS 41

4.1 PRODUCTION COST & OPTIMAL PLANT DIMENSIONS 41

5 DISCUSSION 43

5.1 POWER SERIES 43

5.2 PRODUCTION COST & OPTIMAL PLANT DIMENSIONS 43

5.2.1 Profitability 45

5.2.2 Electrolyser 45

5.2.3 Liquefier 46

5.2.4 Storage 46

5.2.5 Delivery 47

5.3 COSTS 47

5.4 FUTURE PERSPECTIVES 48

5.4.1 Electrolysis technology 49

5.4.2 Liquefaction technology 49

5.4.3 Liquid hydrogen carrier ships 50

6 SUMMARY & CONCLUSIONS 51

REFERENCES: 53

APPENDIX A: FURTHER ANALYSES 55

Abbreviations

AEC	Alkaline electrolyser cell
BEV	Battery electric vehicle
EC	Electrolyser cell
FCEV	Fuel cell electric vehicle
GH2	Gaseous hydrogen
HHV	Higher heating value
LH2	Liquid hydrogen
LHV	Lower heating value
LNG	Liquid natural gas
O&M	Operation & Maintenance
Nm^3	Normal cubic meter (at STP)
PEMEC	Proton Exchange Membrane electrolyser cell
R&D	Research and Development
SOEC	Solid Oxide electrolyser cell
STP	Standard conditions for Temperature and Pressure
WRF	Weather and Forecast model

List of figures

Figure 1.1: Wind map for Norway at an elevation of 80 m (Byrkjedal et al. 2009). 2
Figure 1.2: The regional grid in Varanger, with planned expansions. Source: (Korneliussen 2015). ...4
Figure 1.3: Raggovidda wind farm. Photo: Bjarne Riesto (Teknisk Ukeblad 2015)......5
Figure 2.1: Wind speed distribution at Berlevåg airport in the period from 2005-2014. Data obtained from eklima.met.no (Meterologisk institutt) 8
Figure 2.2: Typical power curve for a wind turbine. 9
Figure 2.3: Global production of hydrogen based on resource. Data obtained from (IHS 2013)......12
Figure 2.4: schematic diagram of an alkaline electrolysis cell (Springer 2014). 15
Figure 2.5: The J-T inversion curve for hydrogen. Sketched after (Tzimas et al. 2003). 18
Figure 2.6: schematic of the liquefaction process. Source: (IDEALHY 2012). 19
Figure 2.7: schematic of a cryogenic vessel. Source: (Linde AG) 22
Figure 2.8: Prototype liquid hydrogen carrier ship. Source: (Kawasaki 2014).....25
Figure 2.9: Mode-map describing the lowest-cost continental hydrogen delivery as a function of transport distance (x-axis, km) and hydrogen flow (y-axis, kg/day). G, L and P indicate compressed gas trucks, liquid trucks and pipelines, respectively. Results from (Yang and Ogden 2007). 26
Figure 3.1: The components of the wind-hydrogen plant......29
Figure 3.2: flow chart of the development process of a time-series of power. 34
Figure 3.3: Correlation between the WRF model (x-axis) and wind data measurements at Raggovidda (y-axis) for the direction bins ranging from 0-30, 30-60, 60-90 and 90-120 degrees. 35
Figure 3.4: Correlation between the WRF model (x-axis) and wind data measurements at Raggovidda (y-axis) for the direction bins ranging from 120-150, 150-180, 180-210 and 210-240 degrees. 36
Figure 3.5: Correlation between the WRF model (x-axis) and wind data measurements at Raggovidda (y-axis) for the direction bins ranging from 240-270, 270-300, 300-330 and 330-360 degrees. 36
Figure 3.6: Comparison of synthesized wind series (red) and measured wind data (blue), moving average daily values......37
Figure 3.7: The power curve of Raggovidda wind farm, based on the method of bins. The standard deviation for each bin is shown......38
Figure 3.8: Comparison of moving average daily values for the measured data at Raggovidda wind farm and the synthesized power series......39

Figure 4.1: Annual costs divided on the plant components, provided an electrolyser capacity of 126.5 MW and 300 tons storage. 42
Figure 5.1: Variation in annual costs and production volume as a function of electrolysis capacity. 44
Figure 5.2: average weekly power input to the electrolysis plant (blue), and the optimal electrolysis capacity (red). 46
Figure 5.3: Storage filling level. Storage capacity shown in red. 47

List of tables

Table 1: wind power in Norway, 2014. Source: (NORWEA and Energi Norge 2015). 3

Table 2: energy density (LHV) of different fuels. Source: (Boundy et al. 2011). 10

Table 3: Heat of combustion, higher and lower heating values, of gaseous and liquid hydrogen. Source: (Tzimas et al. 2003). 10

Table 4: electrolyser data (NEL Hydrogen). 30

Table 5: average exchange rates, January to March 2015. Source: (DnB Markets 2015). 32

Table 6: investment and O&M costs assumed for the components of the plant. 32

Table 7: calculated costs of delivered liquid hydrogen, EUR/kg. The optimal plant dimensions are within the bold frame. 41

1 Introduction

One of the biggest challenges of the world today is climate change. Resulting from the huge amount of greenhouse gases released to the atmosphere during the last century, the average temperature on earth is rising. This is causing disturbances of the climate, which manifest through phenomena like extreme weather, polar ice melting and drought. To restore the balance a green shift is necessary. The heavy dependence of fossil resources must give way to the utilization of renewable energy, and the emissions of greenhouse gases must be significantly reduced.

An increasing portion of intermittent renewable energy in the market cause a demand for energy storage. A fundamental property of the electricity market system is that energy production and demand constantly must balance each other. A widely discussed solution is to store energy in the form of hydrogen. With zero carbon content and a broad variety of production methods hydrogen is a promising energy carrier in the future energy system. It can be converted to power and heat without emissions and with relatively high efficiencies, in mobile as well as stationary applications. It can be used in almost every sector where energy is required, ranging from households and services to transportation and industry (Mueller-Langer et al. 2007). Thus, introducing hydrogen in the energy system can resolve the major concerns about security of energy supply and reduction of greenhouse gas emissions (Tzimas et al. 2003).

To facilitate this highly desired development many governments and international institutions, like for example the United States, Japan and the European Union, has established roadmaps and action plans for hydrogen, see (Agency for Natural Resources and Energy 2014; David et al. 2002; Wurster and Ludwig-Bölkow-Systemtechnik 2008). Since 2001 the Norwegian government have offered tax exemptions and incentives for zero emission vehicles (Riis et al. 2006). On January 29 2015, they also decided to initiate the development of a national hydrogen strategy and stated that all public transport as a main rule shall be emission free in 2025 (Nationen 2015). The Municipality of Oslo and Akershus County Council aims to be among the leading regions in the world for early use of hydrogen for transport solutions. By the end of 2018, the region shall have at least 350 fuel cell vehicles and 30 hydrogen buses (Akershus County Council 2014). 100 % of the public transport in Oslo shall be emission free in 2020.

1.1 Wind power in Norway

As shown in **Figure 1.1**, Norway has got excellent wind resources, especially along the coastline. According to the NVE report 09/2009, (Byrkjedal et al. 2009), Finnmark county has got the highest potential of utilization of wind energy in Norway, due to large exploitable areas with high wind velocities.

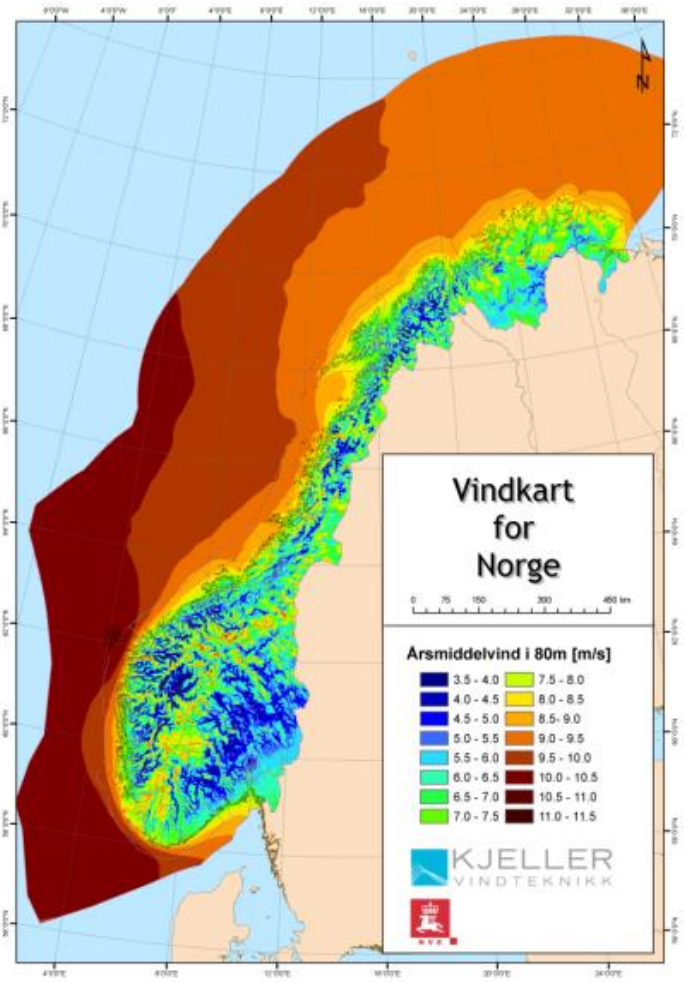

Figure 1.1: Wind map for Norway at an elevation of 80 m (Byrkjedal et al. 2009).

Total production data from 2014 from wind farms in Norway is summarized in **Table 1**. The total capacity is expected to increase substantially within 2020, as a part of the Norwegian-Swedish electricity market, established January 1 2012. As a common goal, the two countries aim at increasing the electricity production by a total of 26.4 TWh from 2012 to the end of 2020.

Installed	856 MW
Production in 2014	2.2 TWh
Capacity factor 2014	31 %
Constructed in 2014	45 MW
Installed expected by 2020	3000 – 3500 MW
Production expected in 2020	6 – 8 TWh

Table 1: wind power in Norway, 2014. Source: (NORWEA and Energi Norge 2015).

The problem of utilizing wind energy is that the favorable resources often are located in areas with a scarce population and thus a weak grid. The development of wind farms is therefore often dependent of grid reinforcements. Such reinforcements require a concession before construction, which is a time consuming as well as an expensive process. However, by using the wind energy for production of hydrogen, grid reinforcements can be avoided. Hydrogen can be stored, utilized locally or distributed by pipelines or cargo tanks, on road, railway or by ship.

1.2 The energy situation in Berlevåg

Berlevåg is a small municipality in Finnmark, the northern most county in Norway. Based on numbers from Statistics Norway, the population amounted to 1042 people in the 3rd quarter of 2013. The annual demand for electricity is about 23 GWh, with a slightly increasing trend (Varanger KraftNett AS 2013).

The regional grid in Varanger, operated by Varanger KraftNett AS, is depicted in **Figure 1.2**. In the top left corner lies Berlevåg, and below is the transformer station Storvarden, which is connected to Raggovidda wind farm. The 66 kV line from Raggovidda to Varangerbotn has a capacity of 55 MW (Korneliussen 2015). Because of a hydropower plant in Kongsfjord of 4.4 MW, the grid capacity for distribution of wind power is about 50 MW.

The central grid, operated by Statnett SF, ends in Varangerbotn, bottom left corner of **Figure 1.2**. The capacity on this 300 kV line is restricted, and according to the Grid Development Plan of 2013 (Statnett SF 2013), Statnett plans the construction of a new line of 420 kV from Ofoten to Varangerbotn. The grid development is divided into four stages, the last one being from Skaidi to Varangerbotn, and Statnett intends to apply for a licence for this stage in 2015. However, there are doubts as to whether or not all four stages are financially profitable, and the progress will primarily be governed by the power demand of new, larger industry (Statnett SF 2013).

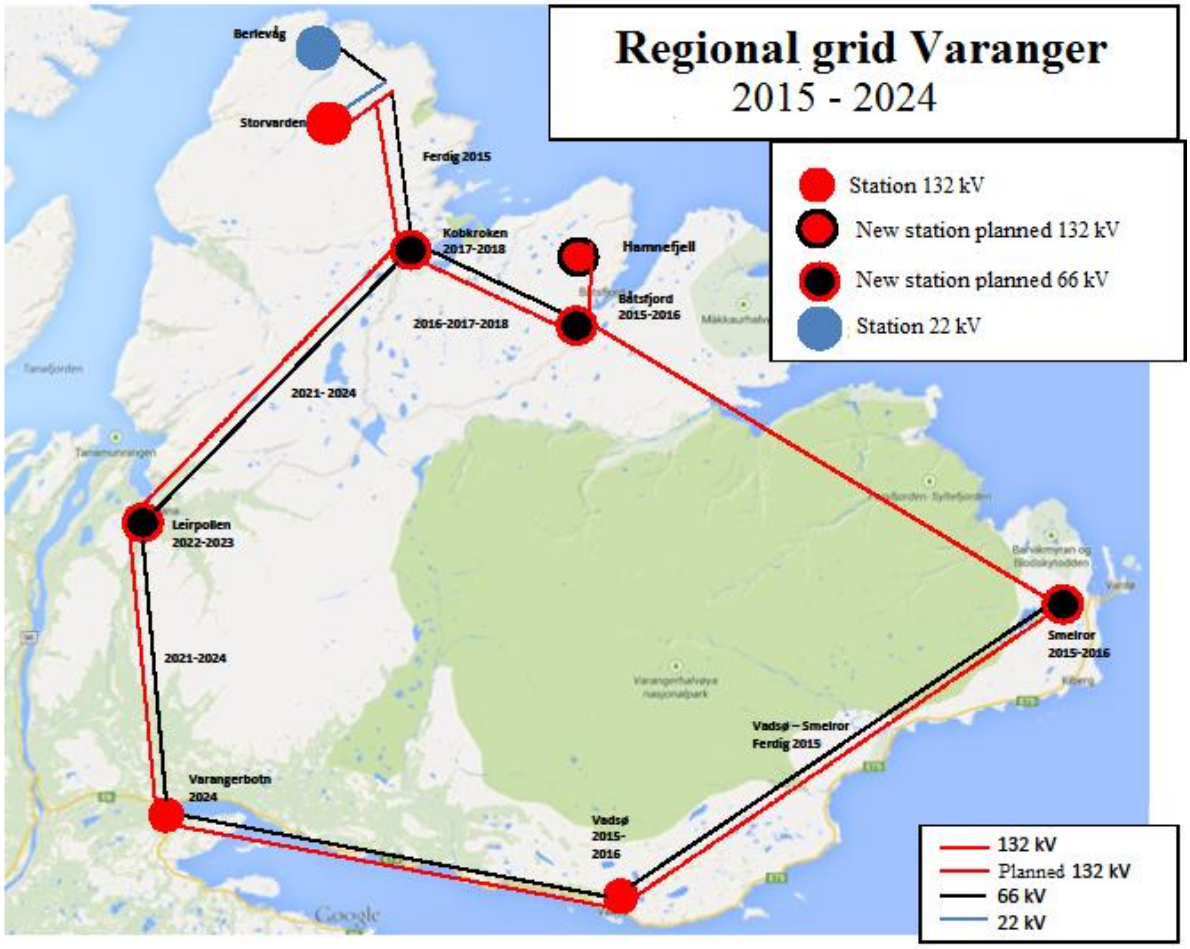

Figure 1.2: The regional grid in Varanger, with planned expansions. Source: (Korneliussen 2015).

Raggovidda wind farm

Raggovidda wind farm is located in Berlevåg municipality and consists of 15 turbines á 3 MW, delivered by Siemens. The hub height of the turbines is 79.5 meters above ground and the wind blades are 49.5 m long. According to Siemens, (Siemens AG 2014), they provide a swept area of 8,000 m^2. The wind farm lies between 380 and 440 meters above sea level in a simple and flat terrain without vegetation.

Raggovidda is given a concession of up to 200 MW, and the first stage of 45 MW was set in operation in September 2014. Because of grid restrictions, it is not possible to distribute more electricity by a potential expansion of the wind farm. An alternative to expanding the grid, now under examination of Berlevåg municipality, is to use the electricity for hydrogen production.

1.3 Scope of the thesis

This master thesis examines the feasibility of hydrogen production with wind power from Raggovidda wind farm in Finnmark. Expansion of the wind farm is currently not possible due to grid restrictions, and hydrogen production is considered an alternative to grid expansion.

The topic is as follows: Provided a full expansion of the wind farm, i.e. 200 MW, and a grid restriction of 50 MW, to what cost may hydrogen be produced from the excess wind power? Which plant size give the lowest hydrogen production cost?

The topic will be approached with computer simulations. A time-series of 20 years of hourly resolution will be synthesized based on a Weather Research and Forecast model, in addition to wind- and production data from Raggovidda wind farm. With the power series as an input, hydrogen production will be simulated in the time domain with Python. The dimensions of the specific components of the plant will be optimized based on a minimization of the production cost of hydrogen.

Figure 1.3: Raggovidda wind farm. Photo: Bjarne Riesto (Teknisk Ukeblad 2015).

2 Background

This chapter introduces the fundamental physics of wind and hydrogen. It provides an overview of the existing technology for the entire chain of a wind-hydrogen plant, ranging from wind turbines to hydrogen production, compression and liquefaction, as well as different storage and distribution methods. Different usage of hydrogen and the current status of the hydrogen market is also introduced.

2.1 Wind power

The energy content of the wind is proportional to the third power of the wind speed. The "available" wind power, P, is defined as

$$P = \frac{1}{2}\rho A v^3 \qquad (2.1)$$

ρ is the mass density of the air, A is the cross-section areas through which the wind is flowing and v is the wind speed. This means that a doubling of the wind speed raises the wind power 8-fold.

The distribution of the wind speeds often correlate with a Weibull distribution. This is shown in **Figure 2.1** for the wind measured at Berlevåg airport in the period from 2005-2014.

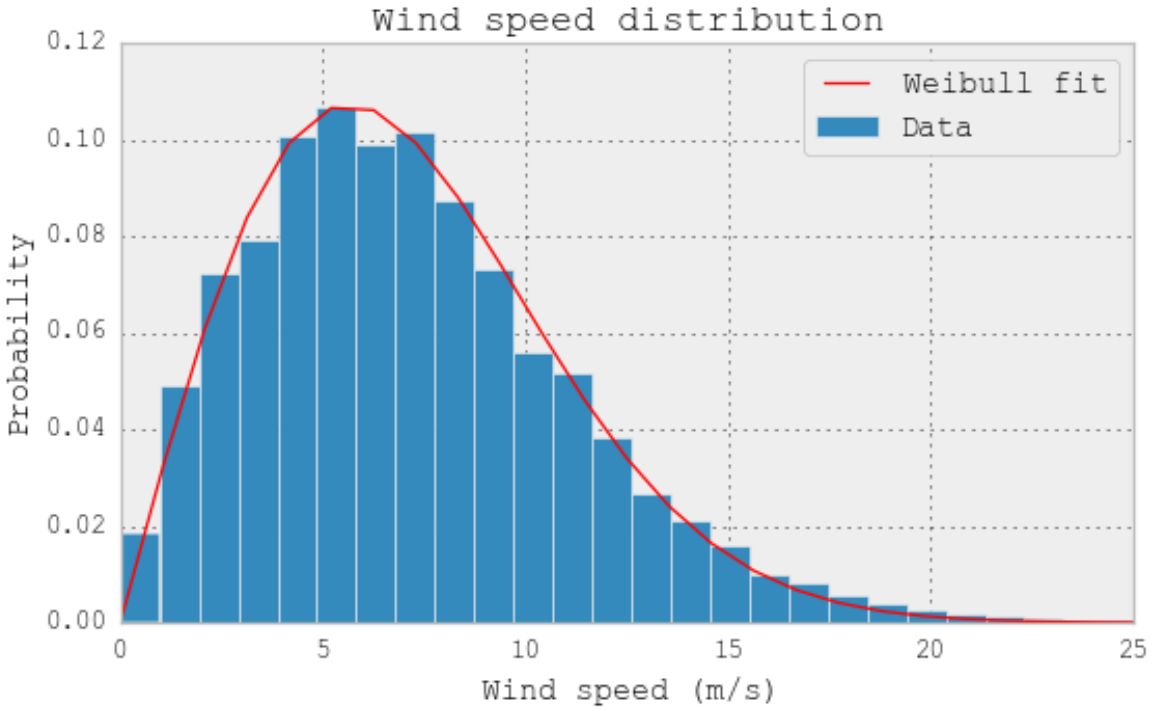

Figure 2.1: Wind speed distribution at Berlevåg airport in the period from 2005-2014. Data obtained from eklima.met.no (Meterologisk institutt)

The average wind speed is 7.2 m/s. However, the median is 6.7 m/s. This is the value of the 50th percentile, which splits the distribution of wind speeds in two equal sized groups of values.

The energy extracted from the wind by a wind turbine can be expressed as the difference in wind speed right in front of and behind the rotor blades. The air cannot come to a complete halt after passing the turbine, and a wind turbine is therefore not able to utilize all of the kinetic energy of the wind. According to Betz law a maximum of 16/27, or 59.3 %, of the available wind energy, as defined in equation (2.1), can theoretically be transformed to mechanical energy in a wind turbine (NORWEA 2012).

Numerous manufacturers of wind turbines exist and a broad range of different technologies are available. However, the selection of the suitable wind turbine is made based upon the wind conditions at the specific site and a target of minimizing the cost of energy produced (NORWEA 2012).

A wind turbine normally starts producing electricity at wind speeds of 3-4 m/s and reaches a maximum power at 11-13 m/s. At higher wind speeds, the power is kept constant by pitching the blades towards lower interaction with the wind. At wind speeds above 25 m/s the wind turbine is shut down. The strain at such high velocities and the risk of break down is too high. A typical power curve for a wind turbine is depicted in **Figure 2.2**.

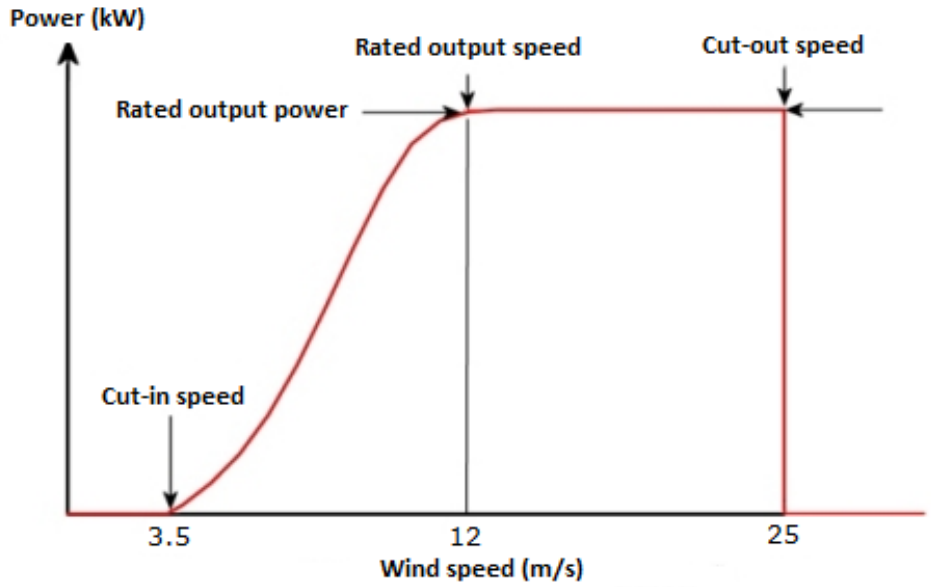

Figure 2.2: Typical power curve for a wind turbine.

Wind turbines are characterized by their installed capacity, which currently in Norway is about 2-3 MW. Over the year, they do not constantly operate at rated power. This depends on many factors, such as wind conditions and maintenance requirements. To compare the performance of different wind farms the ratio between annual produced energy and installed capacity is used. This gives the number of hours the turbine must operate at maximum capacity to produce the annual electricity amount.

$$Operating\ hours = \frac{Annual\ electricity\ produced}{Installed\ capacity} \tag{2.2}$$

By dividing the operating hours by the total number of hours in a year, this ratio can be given as an annual percentage, called the capacity factor.

$$Capacity\ factor = \frac{operating\ hours}{8760} \tag{2.3}$$

The average capacity factor for wind farms in Norway in 2014 was 31 %, see **Table 1**. This corresponds to 2688 operating hours per year.

2.2 Hydrogen

2.2.1 Fundamentals

Hydrogen is the most abundant element in the universe. It has a very low density of 0.08988 kg/m^3 as a gas and 70.8 kg/m^3 as a liquid at standard conditions, STP. On a mass basis, it has an energy content of 33.3 kWh/kg, which is about 3 times higher than other conventional hydrocarbon fuels, as shown in **Table 2**. However, the volumetric energy density is very low. For comparison, a 50 l gasoline tank contains the same amount of energy as a 460 l tank of compressed hydrogen at 350 bar or a 185 l tank of liquid hydrogen (Tzimas et al. 2003).

	Energy density, LHV (kWh/kg)
Hydrogen	33.3
Natural gas	13.1
Gasoline	12.1
Diesel	11.9
Methanol	5.6

Table 2: energy density (LHV) of different fuels. Source: (Boundy et al. 2011).

At normal conditions, hydrogen is in a gaseous state due the low boiling point of -252.87 °C.

In table 3, the higher (HHV) and lower (LHV) heating values of gaseous and liquid hydrogen are compared. The difference between the two values is the latent heat of vaporization of water. Both values express the amount of heat released by complete combustion of a fuel, after the products have been cooled to the initial temperature. However, only the higher heating value accounts for the condensation of produced water vapor. For the LHV the produced water remains in the vapor phase.

	HHV (MJ/m^3)	**LHV (MJ/m^3)**
Gaseous hydrogen (GH2)	12.7	10.8
Liquid hydrogen (LH2)	10040	8490

Table 3: Heat of combustion, higher and lower heating values, of gaseous and liquid hydrogen. Source: (Tzimas et al. 2003).

Hydrogen appears in two different forms, ortho- and para-hydrogen. In ortho-hydrogen the two hydrogen atoms have the same spin, while in para-hydrogen they have opposite spins. Under normal conditions hydrogen consists of 25 % para- and 75 % ortho-hydrogen, but the composition varies with temperature (Tzimas et al. 2003). The amount of para-state hydrogen increases with decreasing temperature, a transition that is exothermic. This is an important phenomenon when liquefying and storing hydrogen, because transitions between the two states result in boil-off losses.

2.2.2 Hydrogen usage

Hydrogen is primarily used as a reactant in the chemical and petroleum industries. By hydrogenation, hydrogen is inserted to saturate or split molecules, to produce lower molecular weight compounds or to remove sulfur and nitrogen. It is mostly used for production of ammonia and refined fuels. Ammonia production accounts for almost 50 % and petroleum processing for about 37 % of the world's total hydrogen demand (Ramachandran and Menon 1998). Other areas where hydrogen is used as a reactant is in plastic recycling, in epitaxial growth of polysilicon and nickel production.

In the nuclear industry hydrogen is used as a O_2 – scavenger to prevent inter granular stress corrosion cracking, which may lead to mechanical failure of the fuel elements. In electrical generators hydrogen is used to reduce friction in rotating armature (Ramachandran and Menon 1998).

Hydrogen may also be used as a fuel in fuel cells, either for mobile or stationary applications. High costs have to date limited this usage to the aerospace industry, but the demand for hydrogen fuel in the transport sector is expected to increase significantly during the next years. Research and development (R&D) has given cost reductions and improvements of the hydrogen and fuel cell technology over the last years. Only during the period from 2005 to 2011 there has been a cost reduction of 83 % for fuel cells (Simonsen 2015a). From 2013, the first mass produced commercial fuel cell electric vehicles (FCEV) were launched to the market, Hyundai being the first with their model Hyundai ix35 Fuel Cell. Toyota launches their FCEV Mirai in 2015 and reports a cost reduction of 95 % compared to the prototype built in 2002 (Dalløkken 2014). Car manufacturers report driving ranges of more than 500 km, refuelling times of about 3-5 minutes, and a fuel cell lifetime of about 10 years (Simonsen 2015a). These features do to a highly extent meet the requirements of the drivers and make fuel cell electric vehicles competitive with conventional petrol or diesel cars. Toyota reports a suggested retail price for Mirai of about $57 500, or about 450 000 NOK in Europe (Toyota Motor Sales 2014).

2.2.3 The hydrogen market

The current global hydrogen production is of 65 million tons per year (Bertuccioli et al. 2014). Of these are only a few percent traded. The majority is produced on-site by large industrial companies to satisfy own demand. Thus, a competitive hydrogen market is not yet established.

As shown in **Figure 2.3**, almost all of the hydrogen currently produced is derived from fossil resources. The majority, 49 %, comes from natural gas reforming, 29 % comes from liquid hydrocarbons and 18 % from coal. Only about 4 % is produced by water electrolysis.

Global spending within the hydrogen and fuel cell technology exceeded in 2008 $5.6 billion (PATH 2011). As the industry grows, the measures of the implementation is unprecise. It is projected that global revenues from the hydrogen and fuel cell industry will lie between $3.2 and $9.2 billion in 2015 and between $7.7 and $38.4 billion in 2020, respectively. By 2050 the industry could grow to as high as $180 billion (PATH 2011).

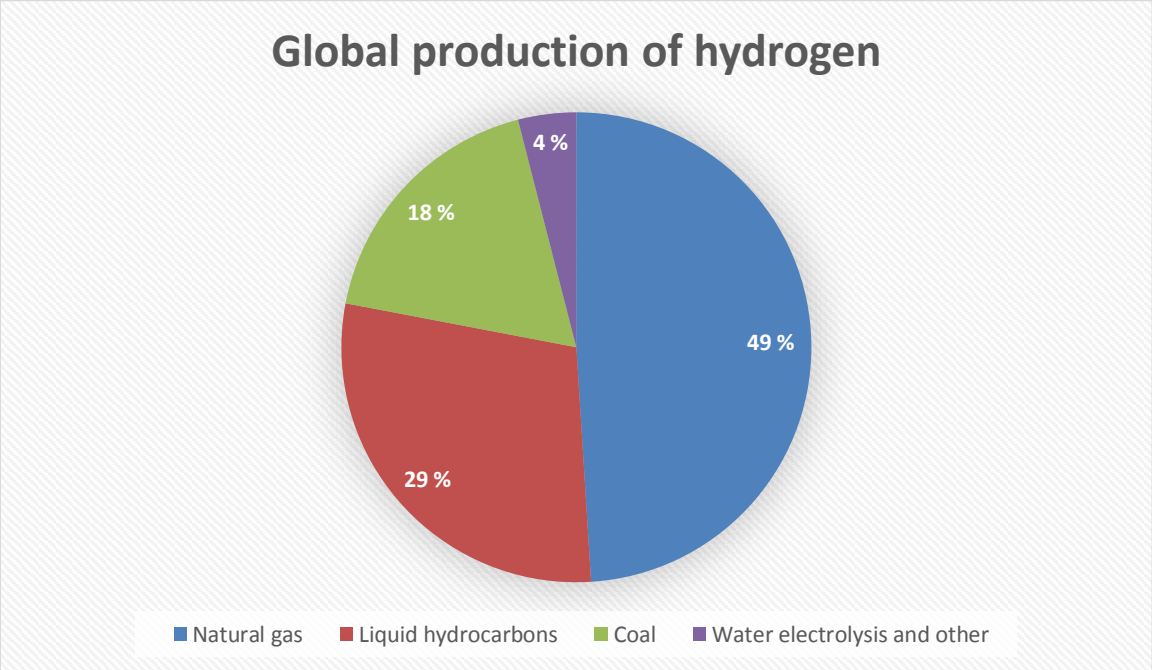

Figure 2.3: Global production of hydrogen based on resource. Data obtained from (IHS 2013).

A competitive market for hydrogen as a fuel for transportation is not yet established. Thus, the charge of hydrogen at refuelling stations is set to a level where parity of fuel costs per km for FCEVs and conventional cars is achieved. In Germany, for example, hydrogen is sold for about 10 EUR/kg (Stolzenburg 2014). In Norway the charge is set to about 90 NOK/kg.

The demand for hydrogen as a fuel for transportation is dictated by the number of fuel cell electric vehicles in use. In 2014, there was 6 hydrogen refuelling stations, 5 hydrogen buses and 20 prototype FCEVs in Norway (Simonsen 2015a).

2.3 The production process

Hydrogen is usually bound to other atoms in compounds. It must therefore be produced, a process that requires energy. There are numerous ways of producing hydrogen, both from fossil and renewable resources, through direct chemical or electro-chemical conversion. Some examples are gasification of coal, steam reforming, direct methanol reforming and water electrolysis (Laguna 2012). The following sections describe various relevant technologies for the entire chain of a wind-hydrogen plant, from electricity to delivered hydrogen. This includes electrolysis, compression and liquefaction, as well as storage and delivery methods.

2.3.1 Water Electrolysis

Water electrolysis is the process where water is split into hydrogen and oxygen by the application of electrical energy. There are many ways of achieving this, but the net reaction is common for the various technologies:

$$H_2O \rightarrow H_2 + \frac{1}{2}O_2 \tag{2.4}$$

The reaction is endothermic, which means that heat must be supplied to keep a constant temperature. The minimum electrical energy required at a given temperature, T, is equal to the change in Gibbs free energy.

$$\Delta G(T) = \Delta H(T) - T\Delta S(T) \tag{2.5}$$

ΔH(T) represents the change in enthalpy and ΔS(T) the change in entropy of the system. The minimum applied cell potential required is called the reversible voltage, U_{rev}, and is related to the Gibbs free energy by the equation:

$$U_{rev} = \frac{\Delta G}{nF} \tag{2.6}$$

n is equal to 2, the number of electrons transferred in equation (2.4), and F is Faradays constant. At room temperature and atmospheric pressure, the reversible cell voltage for water electrolysis is 1.23 V (Springer 2014). The actual cell voltage is however greater than the reversible cell voltage, due to various overvoltages and losses, which may be expressed as follows:

$$U_{cell} = U_{rev} + U_a + U_c + IR \tag{2.7}$$

U_a is the activation overvoltage, U_c the concentration overvoltage and IR ohmic losses. Activation losses are due to resistance to the drive of the chemical reactions, while concentration losses are due to the change in concentration of the gases as they react (Larminie and Dicks 2009d). Ohmic losses are due to resistance to the flow of electrons through the different cell materials, like electrodes and current collectors, and ions through the electrolyte.

The voltage efficiency is defined as the ratio between the reversible cell voltage and the actual cell voltage.

$$\eta_U = \frac{U_{rev}}{U_{cell}} \tag{2.8}$$

U_{rev} is the reversible cell voltage and U_{cell} the actual cell voltage. Equation (2.5) and (2.6) show that the energy demand for water electrolysis decreases with increasing temperature. Changes in cell pressure influences the voltages to a smaller extent, which can be shown by a version of Nernst equation.

$$U_{cell} = U^0_{cell} - \frac{RT}{nF} \ln\left(\frac{1}{\sqrt{p_{H_2} p_{O_2}}}\right) \tag{2.9}$$

U^0_{cell} is the cell voltage at standard conditions, R is the ideal gas constant, n is the number of electrons transferred in equation (2.4), F is Faradays constant, and p_{H2} and p_{O2} is the partial pressures of H_2 and O_2 respectively. At room temperature, providing the partial pressures of the two gases are equal, a pressure change from 1 to 200 bar corresponds to an increase in the theoretical cell voltage of only 34 mV. In theory, higher voltage would infer a greater electricity demand, but increasing pressure gives other positive effects on the overall system operation, as well as reduced costs of compressing hydrogen (Springer 2014).

The currently main existing electrolysis technologies are alkaline electrolysis cell (AEC), proton exchange membrane electrolysis cell (PEMEC) and solid oxide electrolysis cell (SOEC). The main

difference between them is the electrolyte used. An alkaline electrolyser cell use aqueous potassium hydroxide as electrolyte, which conducts ions. In PEMEC the electrolyte is a solid polymer conducting protons, and in SOEC a solid oxide electrolyte conducts oxygen ions under high temperatures.

Because of its technology maturity and demonstrating conversion efficiencies of 64-70 % (LHV) (Mueller-Langer et al. 2007), alkaline electrolysis is considered the best option for hydrogen production in the short and medium term. The future potential of both proton exchange membrane and solid oxide electrolysis technologies should, however, be kept in mind, as they are likely to mature and demonstrate higher efficiencies in the medium term (Mueller-Langer et al. 2007).

Alkaline Electrolysis Cell (AEC)

An alkaline electrolyser consists of two electrodes made of nickel or nickel plated steel immersed in an aqueous potassium hydroxide (KOH) electrolyte, which shown in **Figure 2.4**. The anode and the cathode are separated by a porous diaphragm, through which only hydroxide anions can migrate (Springer 2014).

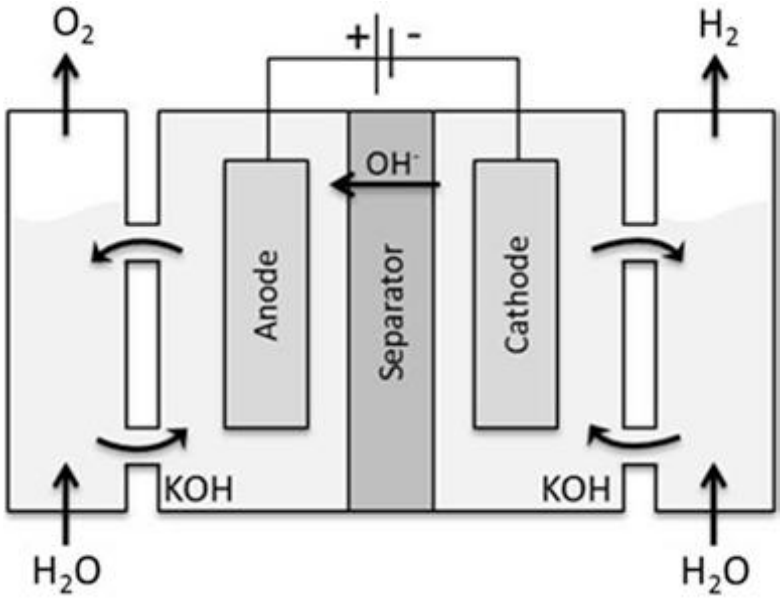

Figure 2.4: schematic diagram of an alkaline electrolysis cell (Springer 2014).

When a direct current is applied to the cell, the following two reactions take place at the electrodes:

Anode: $$2OH^- \rightarrow \frac{1}{2}O_2 + H_2O + 2e^- \quad (2.10)$$

Cathode: $$2H_2O + 2e^- \rightarrow H_2 + 2OH^- \quad (2.11)$$

At the cathode, water is reduced to produce hydrogen and hydroxide ions. The hydroxide ions migrate through the separator to the anode, where they are oxidized to produce oxygen and water molecules. The oxygen and hydrogen is then separated from the electrolyte.

Because water is consumed during cell operation it has to be supplied continuously. The electrolyte is circulated through the cell, but must periodically be refilled due to various types of losses (Springer 2014). A number of cells ranging from 30-200 are connected in series to form a conventional electrolyser stack, with a cell voltage of 1.9-2.4 V. Such a system is normally operated at current densities in the range of 300-500 mA/cm^2 and temperatures of 70-90 °C. The majority of alkaline electrolysers operate at atmospheric pressure and are available at operating pressures up to 25 bars (Riis et al. 2006).

The lifetime of alkaline electrolysers are 7-10 years. Degradation processes, mainly in the catalyst, electrolyte and membrane, lead to an increased cell resistance and thus increased cell voltage during operation. As expressed by equation (2.8), this reduces the efficiency of the electrolyser. Voltage degradation rates typically are in the range of 0.4 – 5 µV/h for state-of-the-art systems under continuous operation (Bertuccioli et al. 2014). After 10 years of operation, assuming a degradation rate of 5 µV/h, the voltage may have increased with 0.44 V, giving an efficiency drop of about 10 %. However, in an electrolyser plant it is not necessary to replace the electrolysers completely. It is possible to replace only the cell stack, i.e. the heart of the electrolyser, giving a good as new component and enabling further operation (Simonsen 2015d). This is called regeneration.

The main advantages of alkaline electrolysis technology are availability, maturity, proven durability and low specific costs compared to other electrolysis technologies. The main challenges are the low current density, low operating pressures and limited modes of dynamic operation. The investment cost of alkaline electrolysers lies in the range of 1,000 – 1,500 EUR/kW (Bertuccioli et al. 2014), and operation and maintenance costs about 4 % of the investment. Regeneration costs lies about 21 % of the initial investment (Simonsen 2015d).

2.3.2 Compression

Due to the low density of hydrogen the compression process requires several stages (Korpås 2004). Usually either piston compressors or centrifugal compressors are used. Although not completely accurate, the hydrogen can be approximated being an ideal gas and the compression process

isothermal, i.e. the temperature is constant during the compression. The theoretical work for isothermal compression of an ideal gas from pressure p_1 to p_2 is given by:

$$W_{1,2} = p_1 V_1 ln \frac{p_2}{p_1} \quad (2.12)$$

p is pressure, v volume and the prefixes 1 and 2 refer to the initial and final state, respectively. The relationship between work and pressure is logarithmic, and the amount of work required to compress hydrogen to the required final pressure is therefore dependent on the initial, suction, pressure. The higher the suction pressure, the lower the energy demand for compression.

This relationship highlights the efficiency advantage of using pressurized electrolysis in the production of hydrogen.

2.3.3 Liquefaction

Liquefaction of hydrogen is achieved by cooling hydrogen gas below its boiling temperature of -253 °C. The process consists of a number of stages, with a wide range of possible technologies and pathways. The hydrogen must be pre-compressed and pre-cooled before leaded through a combination of compressors, heat exchangers, expansion engines and throttle valves. The simplest liquefaction process, the Linde cycle, makes use of the Joule-Thompson effect, as explained in the following.

When a real gas is throttled through an adiabatic valve, the pressure decreases. The temperature, however, may increase or decrease depending on the gas and the initial temperature. This is known as the Joule-Thompson effect. The J-T inversion curve for hydrogen is depicted in **Figure 2.5**. At temperatures below the inversion point expansion will lead to cooling of the gas, while at temperatures above the inversion point expansion will lead to heating of the gas. Therefore, hydrogen must be pre-cooled to a temperature below the maximum J-T inversion temperature, - 69 °C, and pre-compressed to a corresponding pressure on the inversion curve prior to liquefaction.

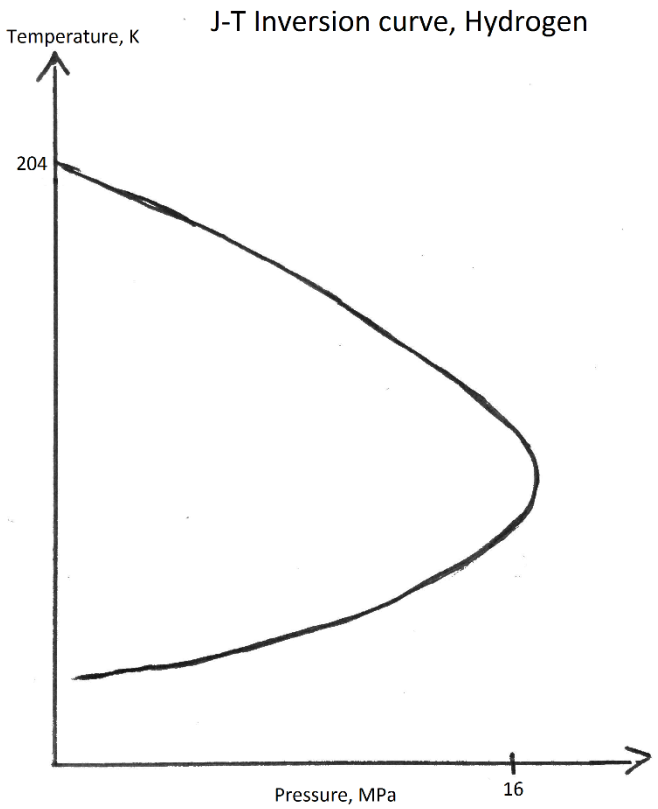

Figure 2.5: The J-T inversion curve for hydrogen. Sketched after (Tzimas et al. 2003).

An alternative to throttling as done in the Linde process, is to pass the high-pressure gas through an expansion engine or turbine. Such an engine will always cool a gas, regardless of its inversion temperature (Amos 1998). However, it cannot be used to condense the gas, because excessive liquid formation in the engine may damage the turbine blades. Using expansion engines, extra heat exchangers and multiple compressors reduces the energy required for the liquefaction process.

To compare the different liquefaction processes a theoretical process called ideal liquefaction is used as a basis. It consists of isothermal compression followed by isentropic expansion to cool and liquefy the gas. The ideal work for the liquefaction of hydrogen is 3.228 kWh/kg (Amos 1998).

Pre-compression and -cooling

The first step of the liquefaction process, as depicted in **Figure 2.6**, is pre-compression and pre-cooling. Hydrogen is pre-compressed to a level of up to 80 bar and then pre-cooled to about 80 K by using nitrogen, hydrocarbons or mixed refrigerants.

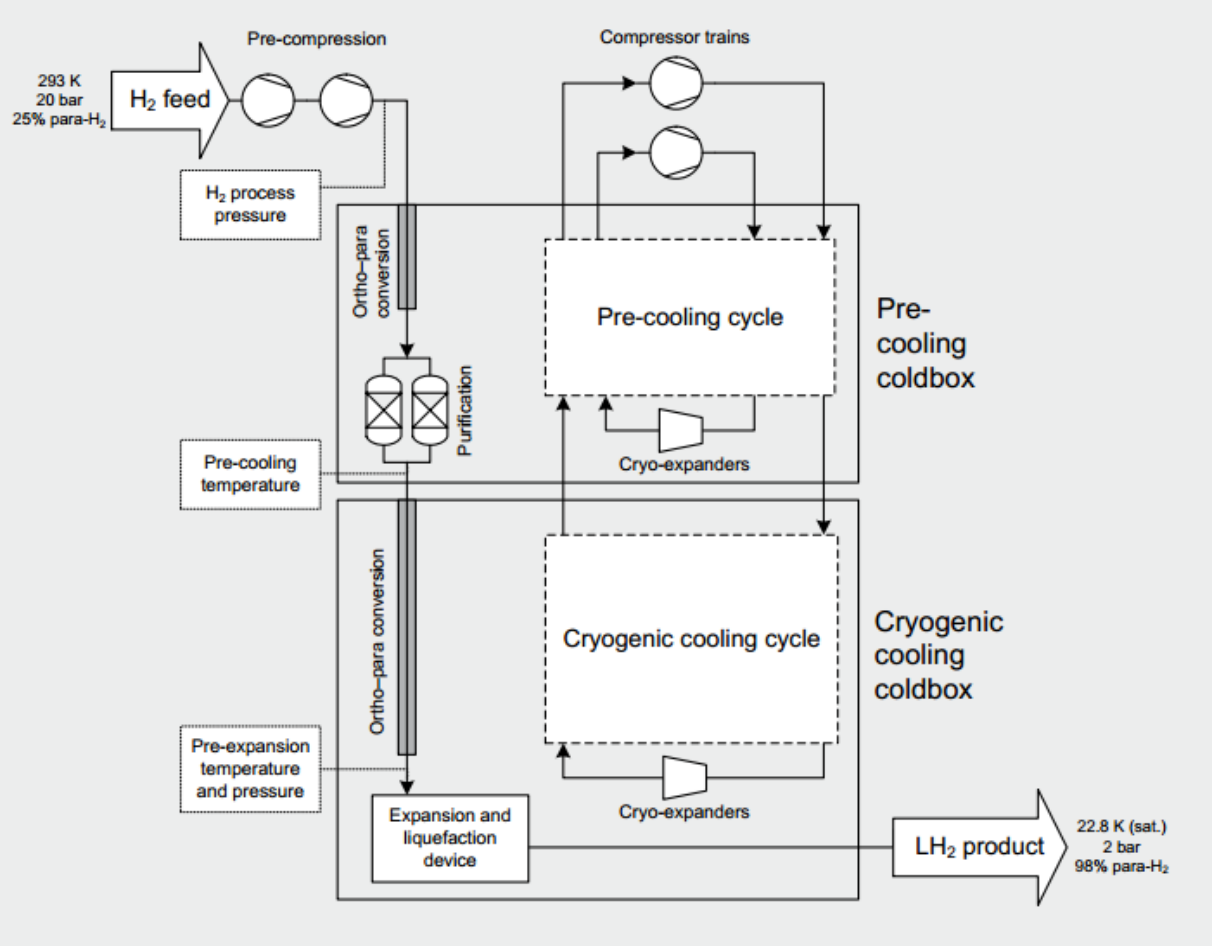

Figure 2.6: schematic of the liquefaction process. Source: (IDEALHY 2012).

Cryogenic cooling

Expanding hydrogen from the inversion point to ambient pressure leads to a maximum decrease in temperature. However, this may not be sufficient to liquefy the hydrogen gas. The cooled gas is therefore heat exchanged with the incoming gas to further reduce the temperature. By repeating the cycle, a low enough temperature is eventually reached such that throttling will lead to the formation of some liquid (Tzimas et al. 2003).

Common liquefaction processes are the Claude cycle, the Linde cycle and the reversible Brayton cycle. Typical refrigerants are helium, neon, hydrogen or a combination of these.

Ortho/para conversion

One of the biggest challenges of liquefying hydrogen is to transform the gas from ortho- to para-hydrogen. If ortho-hydrogen remains in amounts above the equilibrium concentration, it will eventually transform to para-hydrogen, which releases energy and thus increases the temperature. This result in evaporation losses. To ensure a sufficient transformation of the hydrogen states, catalysts, such as iron oxides, rare earth metals and oxides, are used, often embedded in the heat exchangers (Tzimas et al. 2003).

Energy consumption

Liquid hydrogen (LH2) is the most effective way to supply larger refuelling stations, but the liquefaction process is expensive and energy intensive, as well as limited in capacity (Essler et al. 2012). State-of-the-art liquefaction technology typically has an energy consumption of 8-12 kWh/kg LH2 (Amos 1998), which corresponds to about 30 % of the energy content of hydrogen. To improve the efficiency and competitiveness of liquid hydrogen, R&D activities aiming at reducing the energy consumption have been initiated. An example is the EU-funded IDEALHY, Integrated Design for Efficient Advanced Liquefaction of Hydrogen, project. By developing a new process design for LH2 amounts of up to 200 tons per day, it aimed at reducing the specific energy consumption by 50 %, i.e. to a level of about 6 kWh/kg. The project was completed in October 2013, and a large-scale plant for demonstration of the developed technology is under planning.

Costs

The investment costs of liquefaction plants are high, but economies of scale savings are also high. For a 30 tons/day plant the investment cost is about $ 40 million, with a sizing exponent of about 0.57 (Yang and Ogden 2007). The sizing exponent expresses the proportionality between investment costs and capacity:

$$I = I_0 \left(\frac{C}{C_0}\right)^{\alpha} \qquad (2.13)$$

I is the investment cost of the plant component, C is the capacity, α is the sizing exponent and the prefix “0” refers to the base case of the component. A sizing exponent equal to one refers to a linear relationship between investment costs and capacity. A sizing exponent less than one expresses economies of scale for the plant component, giving lower costs per kW for large plant dimensions.

Operation and maintenance (O&M) costs normally lies about 4 % of the investment.

Existing liquefaction plants

In Europe and Asia only a handful of liquefaction plants exist, with a capacity of up to 10.5 tons/day (Tzimas et al. 2003). In North-America there are 10 liquefaction plants, with capacities ranging from 6 to 35 tons/day (Drnevich 2003).

2.3.4 Storage

Due to the expected importance of hydrogen as an energy vector, the research activity on possible storage methods is high (Tzimas et al. 2003). There exist a number of storage technologies, all trying

to address the challenges arising from the low volumetric density and the high diffusivity of hydrogen gas. The following sections introduce some of the most common methods of storing hydrogen, as gas, liquid or a solid.

Compressed gas storage

Storage of hydrogen as compressed gas (GH2) is one of the most common and efficient methods of today (Tzimas et al. 2003). The gas is usually stored in thick-walled cylindrical or spherical steel tanks at pressures ranging from 135 to up to 1000 bar (Hydrogen Delivery Technical Team 2013). Even at such high pressures the density of the gas is very low, and usually less than 2 % of the total storage mass is hydrogen (Larminie and Dicks 2009a). As a result, this method requires large areas. The cost of the compressed gas vessels increases with operating pressure and capacity.

Another challenge of storing hydrogen in pressure vessels is embrittlement. Hydrogen is able to diffuse into the metal, and the gas pressure can build up in internal voids causing stress high enough to crack or blister the steel (Larminie and Dicks 2009a).

An alternative to steel tanks, which are under development and becoming more common, are composite tanks. These are much lighter than steel tanks and thus enable increased storage density and larger transportation volumes. They are impermeable and therefore resistant to hydrogen embrittlement. The main disadvantage is the high cost of the composite materials.

Compressed hydrogen can also be stored underground, such as in large caverns, porous rock or abandoned natural gas wells (Greiner 2010). Such areas provide large storage capacities to much lower costs and are therefore suitable for long-term storage of large amounts of gas. A challenge is the large amount of cushion gas left after a storage cycle, which can be as much as 50 % of the volume (Greiner 2010).

Gaseous hydrogen can also be stored in pipelines, a suitable method for meeting short-term variations in demand (Greiner 2010).

Liquid storage

Hydrogen in liquid form (LH2) has a much higher energy density than hydrogen gas, as shown in **Table 3**. However, the liquefaction process is very energy intensive. This makes LH2 a suitable medium only for storage of large volumes and long transportation distances. In order to liquefy the gas, it must be cooled to a temperature of -253 °C, a complex process that requires a selection of compressors, expanders, heat exchangers and throttle valves, as well as a coolant medium, such as liquid nitrogen. See section 2.3.3 for a more thorough explanation of the liquefaction process.

A gas cooled down to the liquid state is called a cryogenic liquid, and one of the biggest challenges when operating with cryogenics is evaporation due to heat transfer from the surroundings, so called boil-off. For cryogenic liquids this phenomenon cannot be avoided, and the storage vessels are therefore constructed to minimize thermal losses (Tzimas et al. 2003). Even though the pressure normally is of only a few bars, the container is strongly reinforced to withstand pressure buildup due to boil-off. If the pressure exceeds a certain safety level, a spring-loaded valve will release some of the gas. This boil-off may then be collected and re-liquefied (Tzimas et al. 2003). Boil-off rates range from 2 – 3 % per day for small vessels to about 0.06 % for large vessels (Amos 1998).

A cryogenic vessel is typically double walled, and the space between the walls is evacuated to minimize convection and conduction. The shape of the tank is either spherical or cylindrical. Larger storage tanks are often spherical, due to the lower surface area and thus lower evaporation losses. Cylindrical tanks are, however, easier and cheaper to construct (Amos 1998). Capacities range from 6,700 -95,000 L, or 400 – 6,700 kg, of hydrogen (Hydrogen Delivery Technical Team 2013). One of the currently most economical tanks for storing large volumes of hydrogen is the double-wall Horten sphere. It consist of an outer sphere of carbon steel and an inner sphere of stainless steel, separated with 4-inches of perlite (Hydrogen Delivery Technical Team 2013). A cylindrical LH2 container is typically a double-walled vacuum or dewar flask, as depicted in **Figure 2.7**.

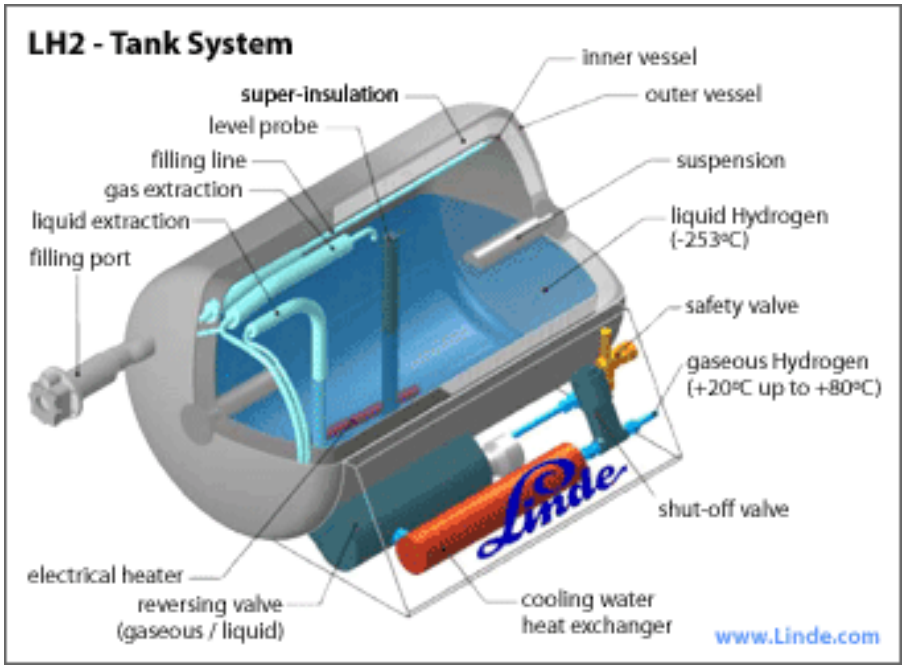

Figure 2.7: schematic of a cryogenic vessel. Source: (Linde AG)

Liquid hydrogen vessels have high capital costs, mostly due to the high insulation required. The cost mainly depends on volume, and for larger tanks the costs range from about 20-40 $/kg hydrogen storage capacity (Yang and Ogden 2007). The sizing exponent, as defined in equation (2.13) is about 0.7, giving significant economies of scale savings for large volumes (Amos 1998). Larger vessels also reduce boil-off losses due to the lower surface area per unit volume.

Solid storage in metal hydrides

A less developed, but promising storage method is the use of metals or alloys, which can act like a sponge absorbing the hydrogen gas and form metal hydrides. The hydrogen atoms bond to the hydrides in a reversible exothermic process, and the gas may later be withdrawn simply by adding heat according to the reaction:

$$M + H_2 \leftrightarrow MH_2 \qquad (2.14)$$

This method can provide high volumetric densities under ambient temperatures and pressures and thereby safety, as well as high efficiencies. Usually several hundred charge/discharge cycles can be completed, depending on the operation conditions. Impurities of the gas may damage the system and very high purity hydrogen must therefore be used (Larminie and Dicks 2009a). Further research is necessary to fully understand the mechanisms of metal hydrides and improve the performance (Tzimas et al. 2003).

Choice of storage

The choice of storage method depends among others on application, storage period and quantity. According to (Amos 1998), storing hydrogen as compressed gas is suitable for small quantities, high cycle times or short storage periods. Liquid storage is suitable for large quantities of gas, long-term storage, low electricity costs or for applications requiring liquid hydrogen.

The capital cost of a cryogenic vessel is lower than that of a compressed gas vessel at capacities in excess of 200 tons of hydrogen. For short-term storage the cost of liquid hydrogen is higher than compressed hydrogen. For longer periods of time liquid storage is cheaper (Tzimas et al. 2003).

An expansion of Raggovidda wind farm to a capacity of 200 MW will result in large production volumes of hydrogen gas. Simulations of the production give an average amount of about 190 tons of GH2 weekly, provided a compressor energy consumption of 2.2 kWh/kg (Amos 1998). A gas truck usually transports about 300 kg of gas, which means that more than 630 trucks would be required weekly. Gaseous production is therefore found unsuitable for the dimensions at Raggovidda.

2.3.5 Delivery

Today hydrogen is mainly used in chemical or petrochemical industries and for this purpose transported via pipelines (Gerboni and Salvador 2009). Numerous other transport methods exist, either by rail, on road or overseas, in cargo tanks, tubes, cryogenic liquid tanks or cylinders. The following section highlights the main transportation methods in use, as well as a future promising solution for delivery over long distances, namely liquid hydrogen carrier ships.

Pipelines

There exist only a limited number of pipelines constructed for hydrogen transport. However, with some modifications it is possible to use the existing natural gas grid for distribution of large amounts of compressed hydrogen gas. The challenge is the low density of the hydrogen gas, which may lead to embrittlement and penetration of valves and seals. Hydrogen leakages may cause explosions. Thus, if pure hydrogen is to be transported in the pipelines, some exposed components, like lubricant and seals, might need replacement. In general, transmission of pure hydrogen in pipelines requires more compression work and have a lower capacity than natural gas for the same energy throughput (Greiner 2010). The actual amount of hydrogen that may be added to the existing gas grid without any modifications is under evaluation, but amounts up to 10 % may be possible. According to Magnus Thomassen, researcher at Sintef, the export capacity in the Norwegian gas grid may range from 5 to 40 TWh (Lie 2013).

Pipeline delivery has very high investment costs, but low operation costs, consisting mainly of compressor power costs (Amos 1998).

It is possible to transport liquid hydrogen in pipelines, but due to high investment and operation costs, this method is preferred for transportation of compressed hydrogen gas.

Trailers

Hydrogen is typically transported in tube trailers for distances in the range of 150 - 300 km. The amount is restricted to about 300 kg GH2 per trailer. For longer distances, up to 1,500 km, cryogenic tanks are preferred (Gerboni and Salvador 2009). A liquid hydrogen trailer can carry up to 4,000 kg of hydrogen (Hydrogen Delivery Technical Team 2013).

Carrier ships

Even though the liquefaction process is expensive, it enables hydrogen to be more efficiently transported over longer distances. Large amounts of liquid hydrogen may be transported on carrier ships in the same manner as liquefied natural gas (LNG). LH2 ships are under development, but have not been built so far. In 2014, Kawasaki Heavy Industries Ltd. was granted the Approval in Principle

from ClassNK for designing and fabricating a cargo containment system suitable on a liquefied hydrogen carrier ship (Kawasaki 2014). The prototype carrier ship developed may carry two cargo tanks, each with a capacity of 1,250 m^3, enabling distribution of up to 177 tons of liquid hydrogen, as shown in **Figure 2.8**. The construction of the ship is planned in the period 2014-2017, aiming at an operation startup in 2017 (Kawasaki 2014).

Figure 2.8: Prototype liquid hydrogen carrier ship. Source: (Kawasaki 2014)

Small scale LNG ships travel at a speed of 12-15 knop (Einang et al. 2005), which enables travelling distances of about 2,000 - 2,500 nautic miles, or 3,700 – 4,700 km, a week. The Norwegian coastline is about 2,532 km in base line, i.e. without fjord and bays (Statistisk Sentralbyrå 2013). It is therefore possible to transport LH2 from Berlevåg to the north of Europe, for example Germany, within a week.

The shipping cost of LNG distribution in Norway is calculated to about 0.40 NOK/Nm^3 for a northern route from Snøhvit to Sandnessjøen with 2 LNG ships of 3,000 m^3 in shuttle (Einang et al. 2005). Terminal costs lies about 50 % of the distribution costs.

Choice of delivery

The favorable and lowest cost method depends on the delivery distance and the amount of hydrogen to be transported. A study from 2007, see (Yang and Ogden 2007), estimated and compared the costs of three different transport methods, namely gas trucks, liquid trucks and pipelines, for varying delivery distances and hydrogen amounts. They found that for short distances and small amounts, gas trucks are preferable. They have low capital investment costs for small gas quantities, but do not

benefit from economies of scale as hydrogen flow increases. The main cost factors are capital costs for trucks and trailers, O&M and fuel costs, which scale linearly with delivery distance. Compressed gas delivery by truck has lower power requirements and slightly lower capital costs than liquid trucks, but the number of tube trailers required to transport the same amount of hydrogen are much higher (Amos 1998).

For medium amounts of hydrogen and long distances, LH2 trucks are thus preferred. The largest cost factors are liquefaction equipment end electricity cost, and the operating costs and truck capital costs are therefore only a small amount of the total (Yang and Ogden 2007). Economies of scale are therefore significant.

For large amounts of hydrogen, pipeline transmission is preferred. The largest cost factor is the pipeline capital costs, which scale strongly with both distance and flow rate (Yang and Ogden 2007). The results are summarized in **Figure 2.9**.

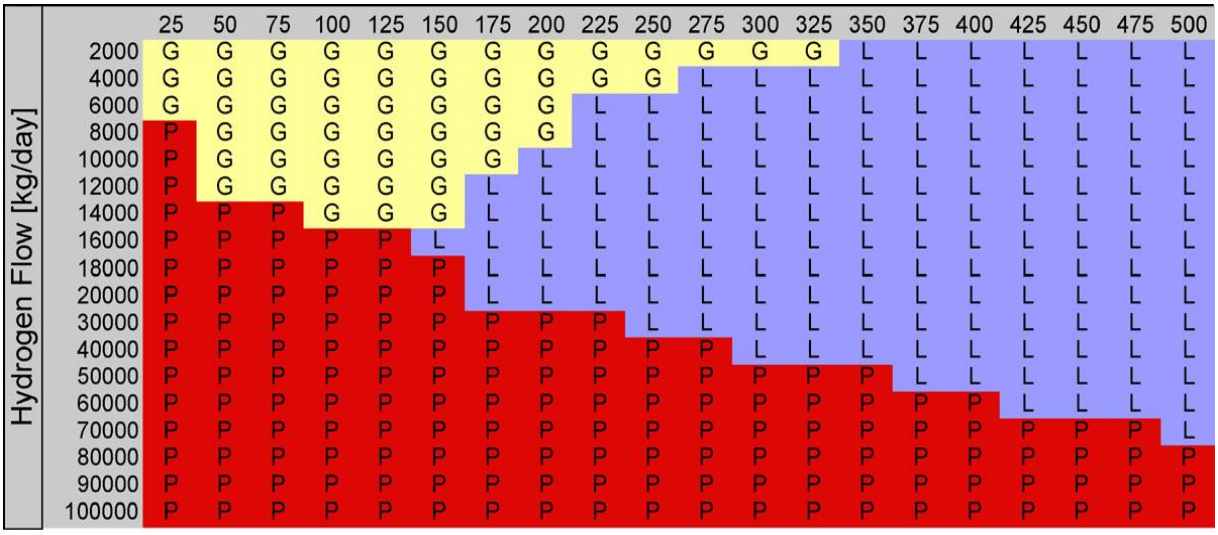

Figure 2.9: Mode-map describing the lowest-cost continental hydrogen delivery as a function of transport distance (x-axis, km) and hydrogen flow (y-axis, kg/day). G, L and P indicate compressed gas trucks, liquid trucks and pipelines, respectively. Results from (Yang and Ogden 2007).

According to (Amos 1998), pipeline delivery is cheaper than all other methods for large quantities of hydrogen, except for transport over an ocean. In that case, liquid hydrogen transport is the cheapest delivery method.

2.4 Economics

The following section gives a brief introduction to the calculation of annual capital costs and production costs.

The annuity factor is defined as

$$a = \frac{i}{1 - (1 + i)^{-n}} \tag{2.15}$$

i is the interest rate per period and n the number of terms.

The annual capital costs are found by dividing the initial investment costs by the annuity factor:

$$Capital\ costs = \frac{I}{a} \tag{2.16}$$

I is the investment cost and a the annuity factor.

The cost of production of hydrogen is found by calculating the annual costs (in Euro) and divide them by the average distributed volume of hydrogen per year (in kg):

$$Production\ costs = \frac{\sum(Annual\ costs)}{Average\ annual\ production} \tag{2.17}$$

3 Methods

Based on data from the operation period of Raggovidda wind farm, a power curve for the turbines is found. A Weather Research and Forecast (WRF) model run by Kjeller Vindteknikk is compared to the measured wind data at Raggovidda. The model is then scaled to better correlate with the measurements, and a wind series is constructed. Eventually, the power curve is combined with the wind series to construct a time-series of power of 20 years with an hourly resolution. This is scaled to a wind farm capacity of 200 MW.

With the constructed power series as an input, the production of hydrogen in a wind-hydrogen plant in Berlevåg is simulated. By minimizing the production cost, the optimal plant dimensions are found.

In the following sections, the methods used in the thesis are explained in detail. Assumptions and simplifications are specified.

3.1 Plant specifications

A lifetime of 20 years and an operation rate of 95 % of the time is assumed for the wind-hydrogen plant. The components of the plant are depicted in **Figure 3.1**. Liquid storage and delivery is considered the best option, due to the large dimensions of the plant.

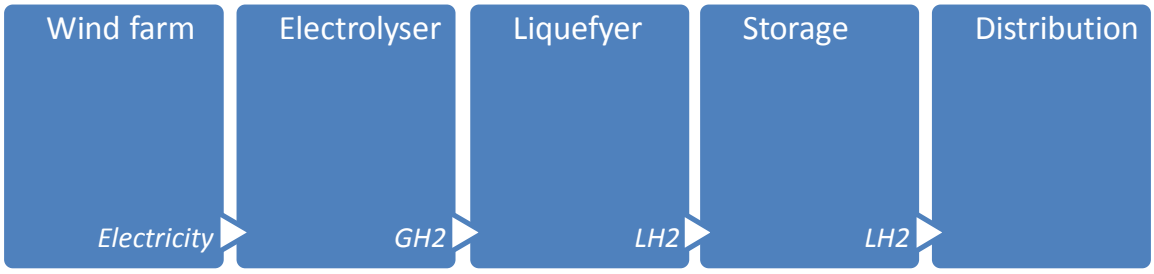

Figure 3.1: The components of the wind-hydrogen plant.

3.1.1 Wind farm

Raggovidda wind farm is assumed being expanded from 45 MW to 200 MW, which means an increase of 155 MW from today's capacity. The grid restriction is set to 50 MW, and power below this level is assumed distributed on the electricity grid. Whenever the wind power exceeds 50 MW, hydrogen is produced.

No losses are assumed for the distribution of electricity from Raggovidda wind farm to the location of the hydrogen production plant.

The power output from the wind farm is expressed as a function of time through the synthesized power time-series.

3.1.2 Electrolyser

Alkaline atmospheric electrolysers of 2.3 MW from NEL Hydrogen are used in the simulations. The total number of electrolysers in the hydrogen production plant is variable, and the total electrolysis capacity is thus a multiple of 2.3 MW. Data for the electrolysers is summarized in **Table 4**.

Nel A-485

Effect	2.3 MW
Capacity	485 Nm^3/h
Energy consumption	49 kWh/kg
Operating temperature	80 °C
Hydrogen purity	99.9 %
Operation range	20 – 100 %

Table 4: electrolyser data (NEL Hydrogen).

Energy consumption by electrolysis depend on the operation load. Since wind power is intermittent, a formula for energy consumption as a function of load is found based on data received from NEL Hydrogen (Simonsen 2015d). The equation found is

$$e_{EC}(l) = 10.85l + 38.07 \qquad (3.1)$$

, where $e_{EC}(l)$ is energy consumption in kWh/kg and l is the part load ratio of full capacity, a number between 0 and 1. For every time-step in the simulations, the part load ratio for the total plant is calculated. All of the electrolysers are thus assumed operating on the same load.

Each electrolyser can operate in the range of 20 – 100 % of capacity. An electrolysis capacity equaling 150 MW wind power corresponds to more than 50 electrolysers. Running only one electrolyser on 20 % corresponds to 0.4 % of total electrolysis capacity of the plant. It is thus assumed that the operation range of the total electrolysis plant is 0 - 100 %.

One electrolyser needs about 7-8 minutes to warm up from stand-by mode and about 30-40 minutes from a cool condition (Simonsen 2015d). Since the simulations are of an hourly resolution, these delays are not taken into account.

Voltage degradation is not included in the simulations. Data on long-term degradation is limited, especially for dynamic operation. Due to the highly dynamic operation, the lifetime of the electrolysers is assumed to be 7 years, after which they are regenerated. During the lifetime of the plant, the electrolysers are thus regenerated twice.

3.1.3 Liquefier

A formula for energy consumption as a function of load is found from data in the IDEALHY report D3.16 (Stolzenburg and Mubbala 2013). The equation is scaled to a full load energy consumption of 10 kWh/kg. This is a somewhat conservative estimate of the liquefier's energy consumption, chosen to also include pre-compression from atmospheric pressure and energy consumption of auxiliaries. The equation found is

$$e(l) = -15.253l^3 + 35.52l^2 - 28.367l + 18.1 \qquad (3.2)$$

, where e(l) is the energy consumption in kWh/kg and l is the part load ratio of full capacity, a number between 0 and 1. The capacity of the liquefier follows from the maximum hydrogen output from of the electrolysers.

3.1.4 Storage

Because of the large wind power capacity at Raggovidda, and thereby large production volumes of hydrogen, liquid storage is considered the best solution. Hydrogen produced is stored in cryogenic dewars and the total storage capacity is variable.

Boil-off losses are assumed a constant rate of 0.06 %/day of total storage capacity (Amos 1998).

3.1.5 Delivery

The storage is assumed emptied once a week, and the LH2 is delivered in two liquid carrier ships in shuttle. The range of the ships is one week of travelling, which corresponds to a distance of 2000-

2500 nautical miles. This resembles delivery of LH2 for example to the northern Europe. The capacity of the ships required follows from the chosen size of the storage.

3.2 Cost calculations

The average exchange rates for January to March 2015 are obtained from DnB (DnB Markets 2015) and summarized in **Table 5**.

	EUR
NOK	0.1144
USD	0.8865

Table 5: average exchange rates, January to March 2015. Source: (DnB Markets 2015).

The investment costs for the different plant components are given in **Table 6**. Installation costs are given as a percentage of the investment costs. The operation and maintenance costs are calculated as a percentage of the investment costs and assumed constant over the entire lifetime of the plant.

	Investment (MEUR/MW)	Sizing exponent	Installation (% of investment)	Annual O&M (% of investment)
Wind farm	1.372	1	20	2
Electrolyser	0.597	1	20	6
Liquefier	2.84[1]	0.57	20	4
Storage	0.84 EUR/kWh[2]	0.7	0	2

Table 6: investment and O&M costs assumed for the components of the plant.

The investment cost of the wind farm expansion is assumed to be 12 mill NOK/MW (NORWEA 2012). Through the procedure described in section 2.4 and a simulation of the mean annual wind power output, this investment is found corresponding to an electricity price of 28.9 EUR/MWh, about 25 NOK øre/kWh. This is a low value, due to the high capacity factor achieved at Raggovidda wind farm, which in the operation period from October 2014 to January 2015 amounted to an average of 55 %.

[1] 30 tons/day plant [2] 300 tons dewar

The expansion of the wind farm also results in increased distribution of electricity on the grid. This extra income is simulated and credited the wind component of the plant.

The investment costs of the electrolysers are assumed to be 12 mill NOK per unit (Simonsen 2015d), corresponding to 1.37 mill EUR. The electrolysers are assumed regenerated after 7 and 14 years of operation, giving an additional investment of 40 %. These reinvestment costs are assumed equally distributed over the 20 years of operation, giving an extra annual cost of 2 % of the investment, and then added to the O&M costs. Normally, O&M costs for electrolysers lie about 4 % of the investment and in this case, including reinvestments, they thus amount to 6 %.

The investment costs of the liquefier is assumed to be $ 40 million for a 30 tons/day plant, which for a specific energy consumption of 10 kWh/kg corresponds to 2.84 EUR/MW. A sizing exponent of 0.57 is assumed, and O&M costs are assumed to be 4 % of the investment.

The storage costs are assumed 8.36 million EUR for a 300 tons dewar, with a scaling factor of 0.7. O&M costs are assumed 2 % of investment.

In addition to the values in Table 6, delivery costs must be considered. Since LH2 carrier ships are under development, few sources were found on costs of oversea delivery of hydrogen. As a basis, shipping costs for LNG distribution in Norway is used. As mentioned in section 2.3.5, this amounts to about 0.40 NOK/ Nm^3 LNG. This corresponds to about 0.54 NOK/kg LNG, provided 1 Nm^3 of natural gas weighs 0.735 kg. 1 m^3 of LNG weighs 450 kg, which gives a specific volumetric cost of 245 NOK/m^3 liquid gas. Assuming the LNG ships may deliver an equal volume of liquid hydrogen as LNG, the delivery cost corresponds to about 0.4 EUR/kg LH2. To account for the probable higher investment costs for the newer technology of liquid hydrogen carriers, as well as terminal costs of loading and unloading the hydrogen, the cost is multiplied with two, giving a delivery cost of 0.79 EUR/kg.

An interest rate of 5 % is chosen based on the weak global economic situation. By equation (2.15) and (2.16), provided a plant lifetime of 20 years, the annuity factor is calculated to be 12.46 and the annual capital costs thus amounts to 8 % of the total initial investments.

3.2.1 Electricity income

Compared to today's electricity distribution, an expansion of Raggovidda wind farm from 45 MW to a capacity of 200 MW will cause increased sales of electricity. This do not directly influence the hydrogen production cost, but do make the investment in the wind farm expansion more profitable.

To account for the extra income, the annual extra income from electricity sales from wind power below 50 MW is thus subtracted from the annual capital costs. Thus, the annual wind costs consist of investment costs, O&M costs and electricity sales.

Based on data obtained from Nord Pool Spot (Nord Pool Spot 2015) the average elspot price in Finnmark for the last 12 years are found to be about 40 EUR/MWh, or 35 øre/kWh. Based on NVE's report on elcertificates for the 4th quarter of 2014 (NVE 2015) an average certificate price of 19 EUR/MWh is assumed.

The annual electricity production of a 200 MW expanded wind farm at Raggovidda, as well as for the current 45 MW farm is simulated based on the synthesized power series. Only electrical power up to 50 MW is delivered to the electricity grid. The difference in distributed electricity between the two stages of the wind farm is calculated, and the annual extra income from electricity sales due to the expansion of the wind farm is found.

3.3 Development of a time-series of power

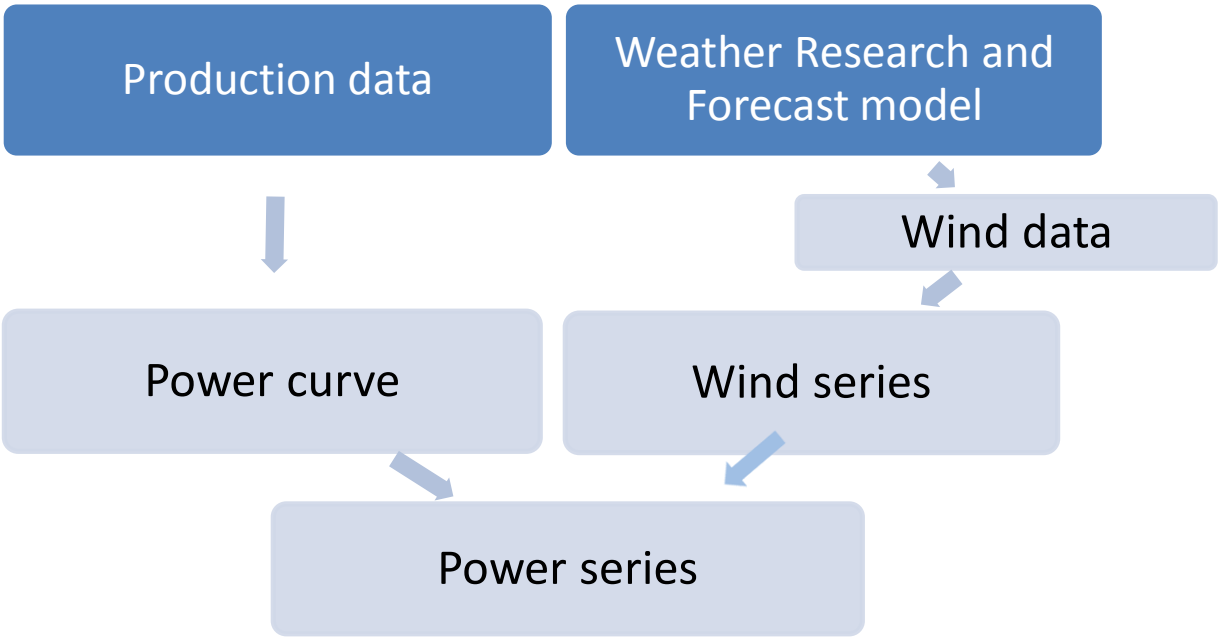

Figure 3.2: flow chart of the development process of a time-series of power.

Based on data from the operation period of Raggovidda wind farm, a power curve for the turbines is found. A Weather Research and Forecast model run by Kjeller Vindteknikk is compared to the measured wind data at Raggovidda. The model is then scaled to better fit the measurement, and a wind series is constructed. By combining the wind series and the power curve a power series of 20

years of hourly resolution is constructed. The following section explains this process, as illustrated in **Figure 3.2**, in detail.

3.3.1 Wind series

A long-term wind speed time-series is constructed based on a Weather Research and Forecast (WRF) model run performed by Kjeller Vindteknikk. WRF is a mesoscale meteorological model used for both research and weather forecasting. For application in this thesis, a model is run with 4 km x 4 km and hourly resolution over the period from 2000 to 2014. The model data is run at an altitude of 113 m above ground, and later scaled to the hub height of 80 m.

The model is compared with wind data measurements at Raggovidda. Data from August and September is considered uncertain due to start-up testing of equipment. This period is thus disregarded, and only data from October 2014 to January 2015 is used. The WRF model is somewhat adjusted to better fit the measured wind data. This is done by dividing the two series into 12 equal sized bins based on wind direction and compare the values. A correlation factor is then found for each direction, as depicted in **Figure 3.3** - **Figure 3.5**.

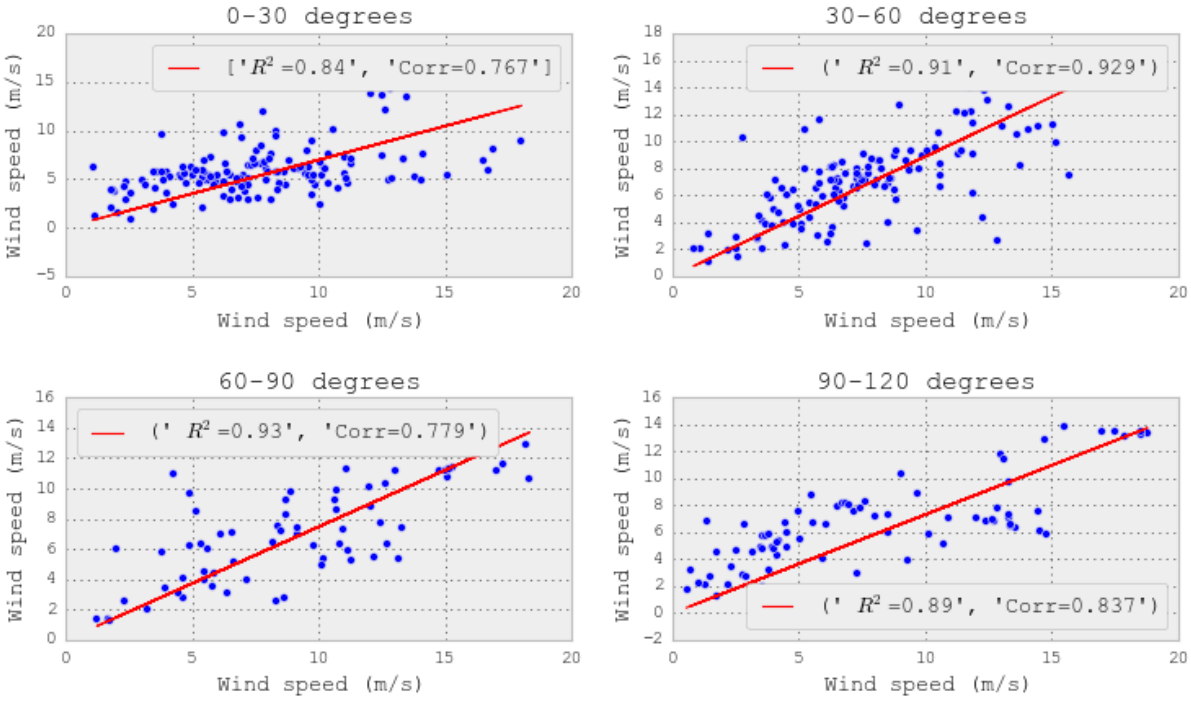

Figure 3.3: Correlation between the WRF model (x-axis) and wind data measurements at Raggovidda (y-axis) for the direction bins ranging from 0-30, 30-60, 60-90 and 90-120 degrees.

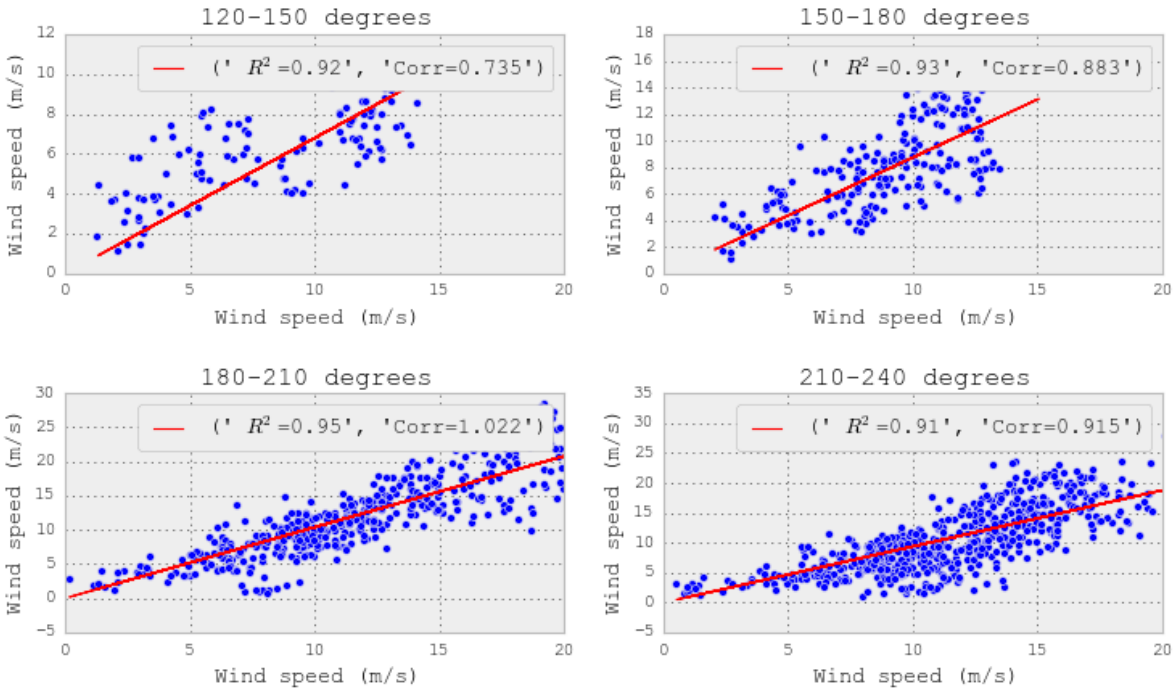

Figure 3.4: Correlation between the WRF model (x-axis) and wind data measurements at Raggovidda (y-axis) for the direction bins ranging from 120-150, 150-180, 180-210 and 210-240 degrees.

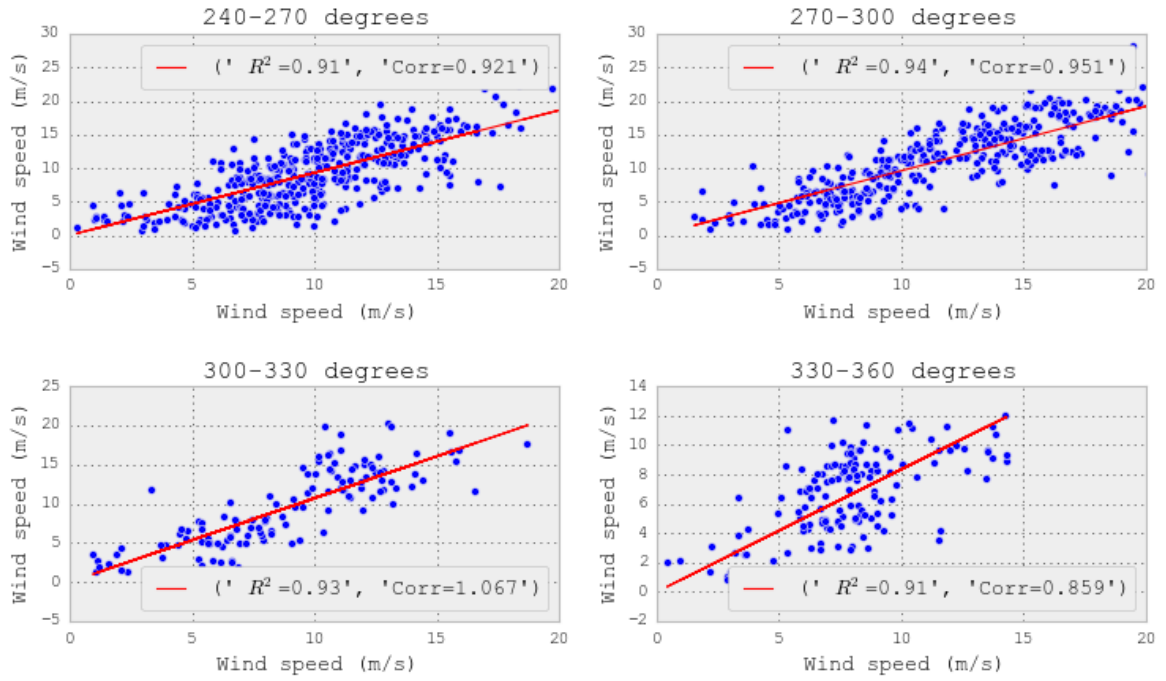

Figure 3.5: Correlation between the WRF model (x-axis) and wind data measurements at Raggovidda (y-axis) for the direction bins ranging from 240-270, 270-300, 300-330 and 330-360 degrees.

The WRF model is scaled with the correlation factors found for each wind direction bin, and a time-series of wind velocities is thereby synthesized. This wind series is compared with the wind data measured at Raggovidda and found to correlate well in the operation period of the wind farm, as depicted in **Figure 3.6**. The correlation factor between the series during the operation period from October 2014 to January 2015 is 0.8.

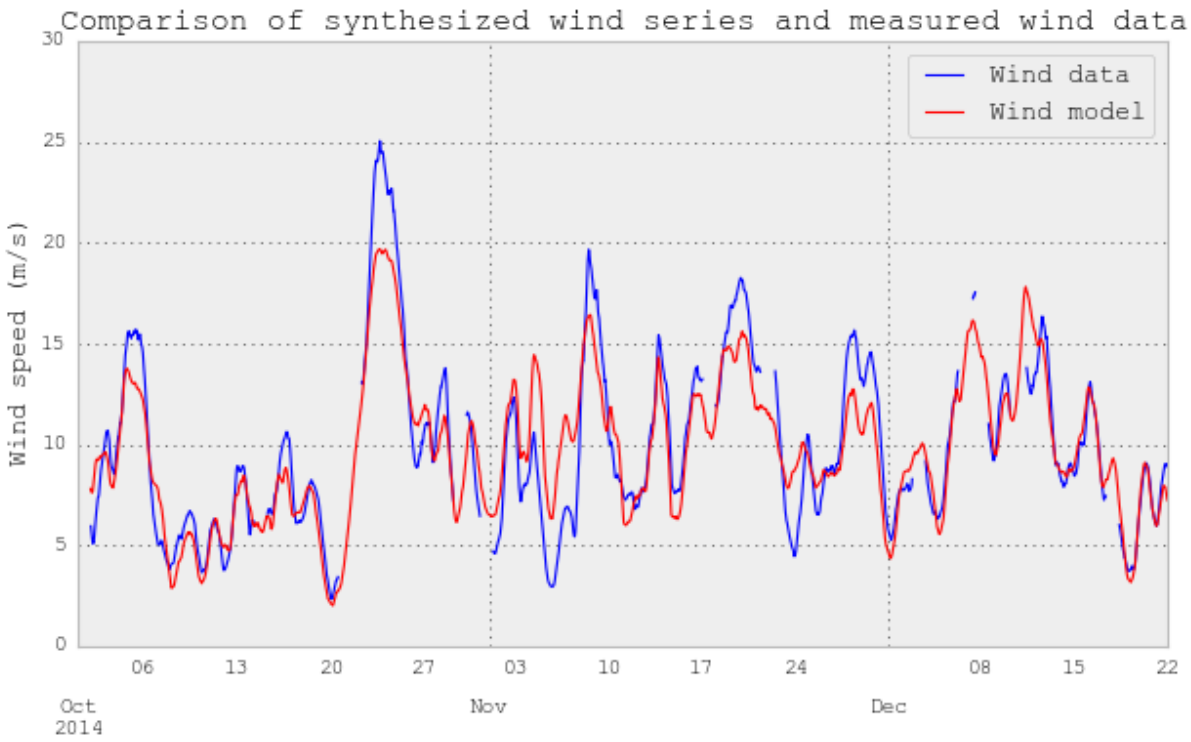

Figure 3.6: Comparison of synthesized wind series (red) and measured wind data (blue), moving average daily values.

3.3.2 Power series

The power curve for Raggovidda wind farm is found with three different approaches. Based on the theory from chapter 2.1 a third degree polynomial is customized using regression on the production and wind data from the operation period (October to January). Another power curve is found based on the method of bins. The measured production and wind data series are grouped into wind velocity bins of width 1 m/s, giving bins from 0-1 m/s, 1-2 m/s and so on. The average power from the operation period is then found for each bin, as depicted in **Figure 3.7**, and a continuous power curve is drawn by interpolating between the values. A third approach utilizes the method of bins on the production data and the scaled WRF model. For every time step in the operation period, October to January, each wind velocity of the scaled WRF is assigned the corresponding power output from the production data. The series is then grouped into velocity bins of width 1 m/s, and the average

power of each bin is found. By interpolating between the values, a continuous power curve is constructed.

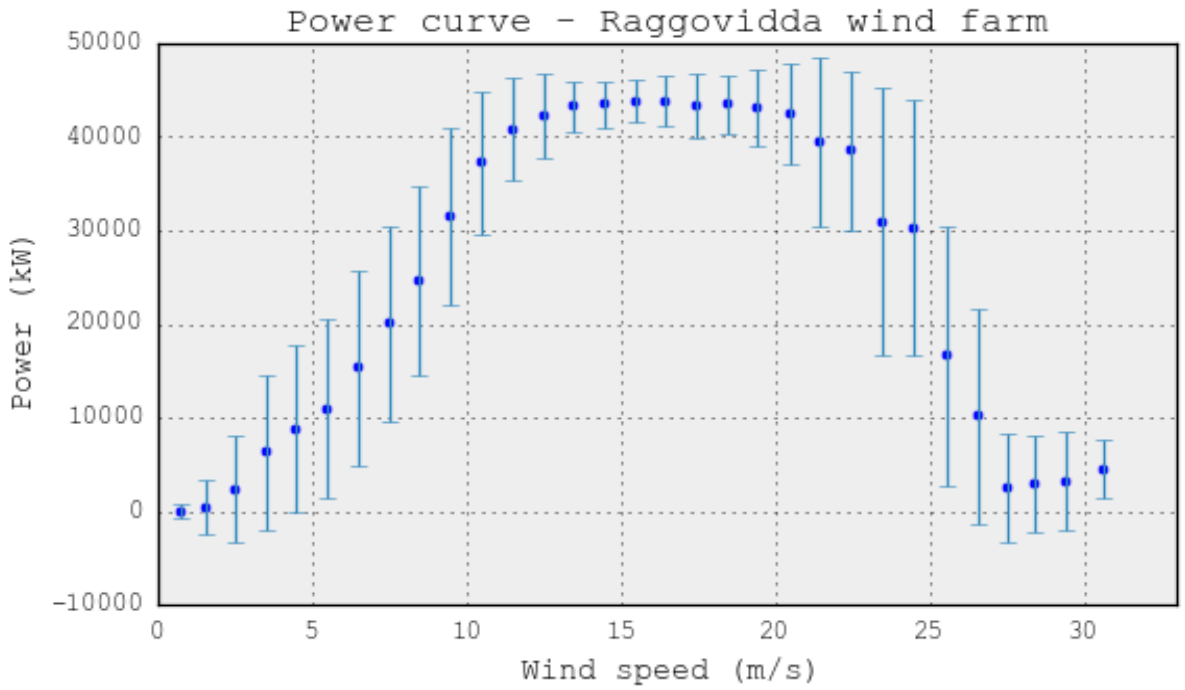

Figure 3.7: The power curve of Raggovidda wind farm, based on the method of bins. The standard deviation for each bin is shown.

To synthesize a continuous time-series of power the power curves are used on the scaled WRF wind series. Every wind speed of the series is assigned a corresponding power output from the wind farm, and for each of the three approaches power series of hourly resolution from 2000 to 2014 are constructed.

Eventually, the power series are analyzed and compared with the power production data from Raggovidda wind farm. The method of bins based on wind data, method number two, is found to correlate well with the production data and is therefore chosen for the further simulations. For the operation period of October to December 2014, a correlation factor of 0.76 is obtained. A comparison of the moving average daily values of the two series are depicted in **Figure 3.8**. To obtain a series of 20 years length, the first 5 years are repeated and added to the end of the series.

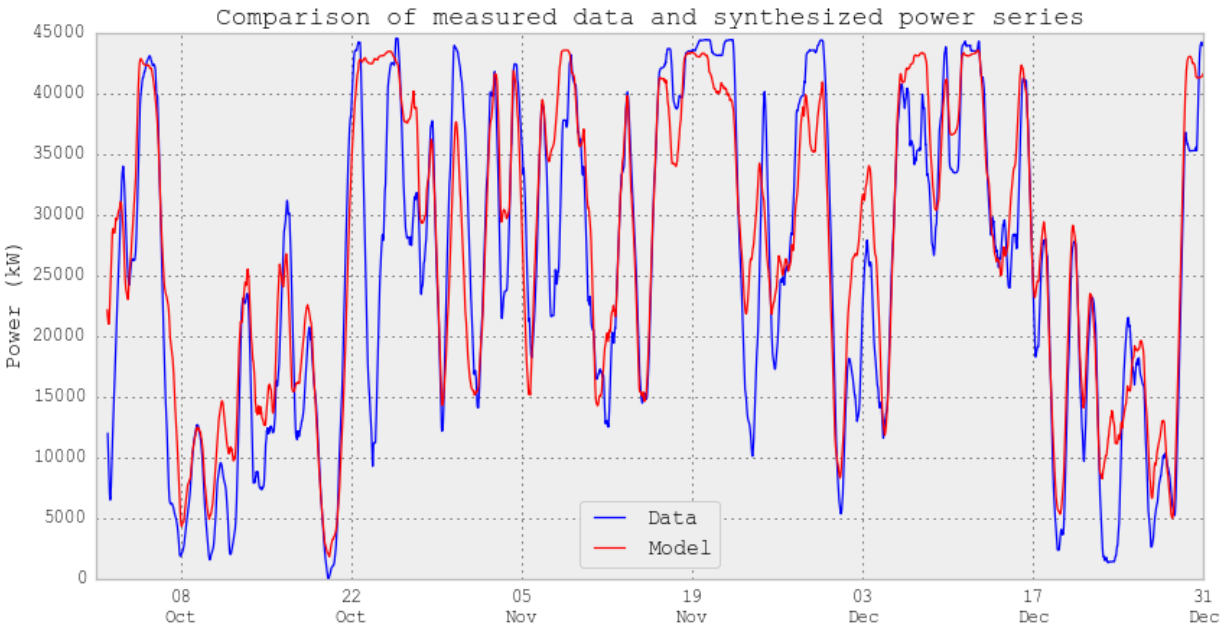

Figure 3.8: Comparison of moving average daily values for the measured data at Raggovidda wind farm and the synthesized power series.

3.4 Plant simulations

As a simulation tool, Python with the open-source library Pandas, has been used. With the developed power series as an input, the production of hydrogen is simulated in the time domain. Electricity is assumed converted to liquid hydrogen momentarily, with no lagging between the electrolysis and liquefaction components.

By minimizing the production cost of hydrogen, the optimal plant dimensions are found. The electrolysis and storage capacity are selected as design variables. The required capacity of the liquefier follows from the maximum output of hydrogen from the electrolysers, while the required capacity of the liquid carrier ships follows from the maximum storage capacity chosen.

4 Results

A time-series of wind power of 20 years of hourly resolution is synthesized as described in section 3.3. With this as an input, the production of hydrogen is simulated, and the plant components are optimized by minimizing the production cost of hydrogen.

4.1 Production cost & optimal plant dimensions

Based on the assumptions in section 3.2 and equation (2.17), the production costs as a function of electrolysis and storage capacity are found. The liquefaction capacity required follows from the maximum hydrogen output of the electrolysers and delivery capacity required follows from the storage capacity. The results are summarized in **Table 7**.

Storage (tons) / EC (#)	400	300	200	100
66	4.31	4.34	4.85	7.39
55	4.24	4.23	4.57	6.79
45	4.33	4.30	4.42	6.25
35	4.57	4.52	4.49	5.77
25	5.08	5.02	4.95	5.44
15	6.45	6.35	6.24	6.13

Table 7: calculated costs of delivered liquid hydrogen, EUR/kg. The optimal plant dimensions are within the bold frame.

The optimal combination found is 55 electrolysers and 300 t weekly storage of LH2. This combination was found to give the lowest production cost per kg hydrogen delivered, amounting to 4.23 EUR/kg. Provided a 5 % result cost interval, the optimal dimensions range between 103.5 – 151.8 MW electrolysis capacity and 300 – 400 tons storage capacity, giving a production cost of up to 4.34 EUR/kg.

For the optimal plant dimensions, the annual costs divide on the different components of the plant as depicted in **Figure 4.1**. The electrolysis component constitute the majority of the annual costs, amounting to 33.9 %. The costs related to the wind farm expansion constitute 29.7 % of the costs, after subtracting the extra income from the increased electricity distribution on the grid. The liquefier constitutes 15.3 % and delivery 18.7 %. The lowest costs are those related to storage, which amount to only 2.4 % of the annual costs.

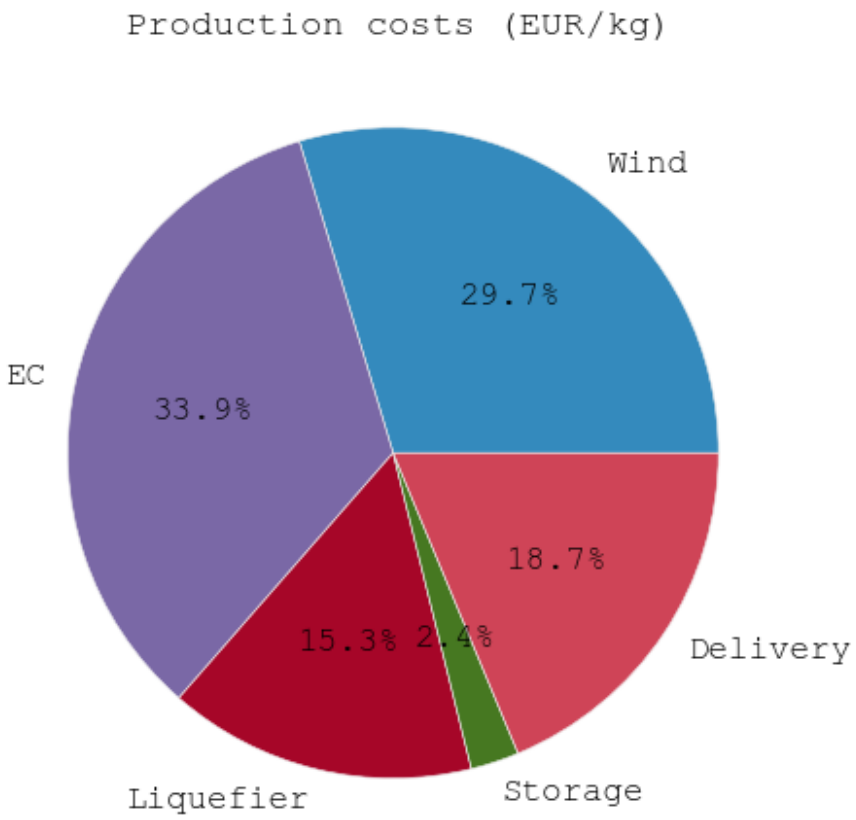

Figure 4.1: Annual costs divided on the plant components, provided an electrolyser capacity of 126.5 MW and 300 tons storage.

5 Discussion

5.1 Power series

The correlation factor between the wind measurements at Raggovidda and the constructed wind series during the period from October to December 2014 is found to be 0.82. Between the synthesized power series and the production data, a correlation factor of 0.76 is obtained.

While the wind data consist of 10-minute intervals, the wind series is of an hourly resolution. Fluctuations within the hour are therefore lost. This is, however, considered acceptable, because of the much smoother characteristics of the wind power output from the wind farm.

By using the WRF model, it is assumed that the wind speed is constant over the entire farm area, i.e. every wind turbine is subject to the same wind speed. In reality, the local variations in wind speed may be significant. At high wind speeds, some wind turbines may be shut down while others continue in operation. This is what causes the descending shape of the power curve for high wind speeds, as depicted in **Figure 3.7**, which contrast to the theory in chapter 2.1 and **Figure 2.2**.

Occasionally, the wind speed is so high that the entire wind farm is shut down. This effect is not covered by the constructed power series, because of the descending power curve for high wind speeds. When the farm in reality is shut down, the constructed power series may give a theoretic power output.

The power series also excludes some of the peak production periods. This can be explained by the wind model, which for high wind speeds has larger deviations. As seen in **Figure 3.7**, the error bars of the power curve are largest for wind speed between 23 and 27 m/s. This correlate with the wind speeds for which the wind turbines may be shut down.

To cover the variation in power output within each velocity bin in the power curve model, a normal distribution within each bin based on the standard deviations could have been applied. This would have given a more dynamic power series.

5.2 Production cost & optimal plant dimensions

The optimal dimensions of the plant is found to be 55 electrolysers, i.e. an electrolysis capacity of 126.5 MW, and 300 t weekly storage of LH2. This was found to give the lowest production cost per kg hydrogen delivered, which amount to 4.23 EUR/kg. Provided a 5 % result cost interval, the optimal

dimensions range from 103.5 – 151.8 MW electrolysis capacity and 300 – 400 tons storage capacity, giving a production cost of up to 4.34 EUR/kg.

The optimal electrolysis capacity corresponds to 84 % of maximum wind power. This results in about 10 % reduction of the production volume compared to a case where the electrolysis capacity equals the maximum wind power of 150 MW.

To explain the optimal range of plant dimensions, the variation in production volume and annual costs as a function of electrolysis capacity has been found, as depicted in **Figure 5.1**. All plant component capacities follows here from the maximum hydrogen output from the electrolysis. All values of the production volume and annual costs are given as a percentage of the case where electrolysis capacity equals wind power capacity, so called "wind power scale". It is seen from **Figure 5.1** that for an electrolysis capacity between 100 – 150 MW the annual costs and production volume are about equally reduced, giving the lowest production costs per kg hydrogen. Where the difference between reduction in production volume and annual costs are largest, the minimum production cost is found.

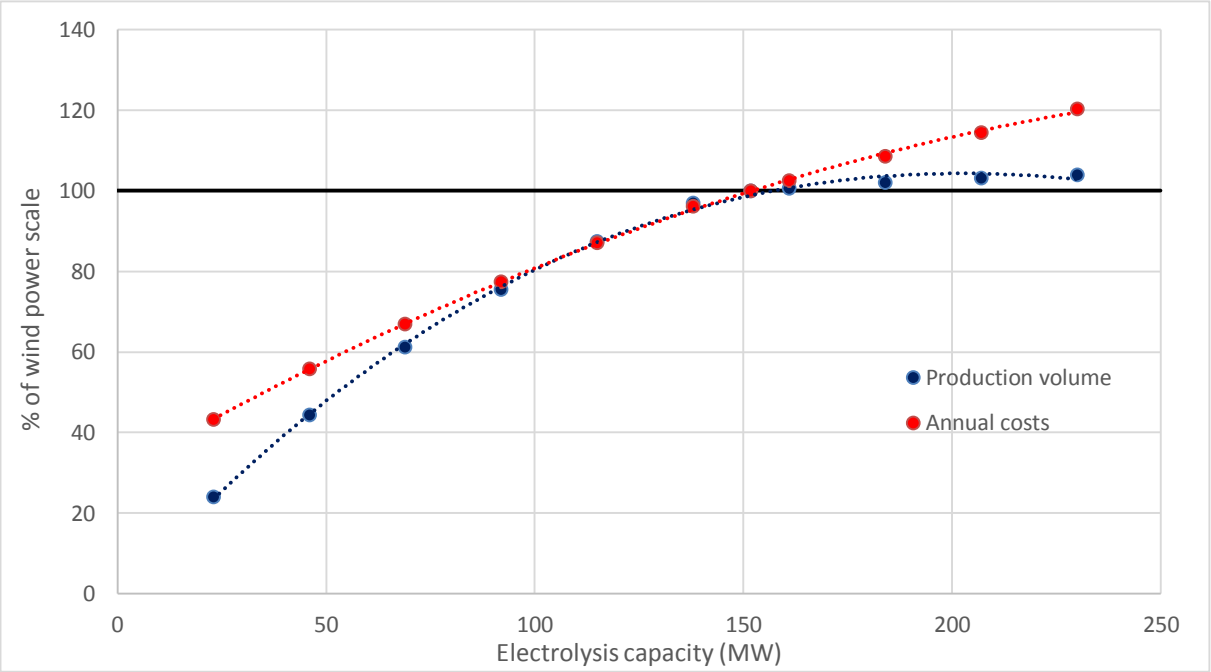

Figure 5.1: Variation in annual costs and production volume as a function of electrolysis capacity.

An over-dimensioning of the plant would give a higher production volume than for the optimal dimensions found, but increased investment costs result in higher production costs of hydrogen. On

the other hand would a small wind-hydrogen plant require lower investments, but the low production volumes make such a plant less profitable.

The variations in the production costs for the different plant dimensions are small. This can be explained by the resembling variations in annual costs and production volume. Both can be approximated by polynomials, and for an electrolysis capacity ranging from 100 – 150 MW, the variations in annual costs and production volume are almost equal.

Another important factor for the results is the dominating investment cost of wind power, which is constant and constitutes about 30 % of the annual costs.

5.2.1 Profitability

A production cost of 4.23 EUR/kg LH2 is found, corresponding to about 37 NOK/kg. Currently, the charge of hydrogen at refuelling stations is set to a level where parity of fuel costs per km for fuel cell electric vehicles and conventional cars is achieved. In Norway, hydrogen is sold at refuelling stations at a charge of 90 NOK/kg, and in Germany hydrogen is sold for about 10 EUR/kg. Thus, a revenue of more than 5 EUR/kg hydrogen may be achievable, provided no VAT or taxes are added.

5.2.2 Electrolyser

The average wind power input to the electrolysis plant is found to be 62 MW, which is about 49 % of the optimal electrolysis capacity found. The simulated weekly average power input to the electrolysers and the optimal electrolysis capacity is compared in **Figure 5.2**.

The production of hydrogen may be increased by optimizing the operation of the electrolysers. In the simulations they are run at the same load, ranging from 0 – 100 %. However, in reality some of the electrolysers may be shut down while others remain in operation, to optimize production and lower production costs.

The energy consumption of the electrolysers is expressed through a linear relationship with varying part load. The equation is found based on an approximation to data from (Simonsen 2015d). Generally, the efficiency of electrolysers is largest for a part load of about 70-80 % of capacity. However, my approximation expresses a linear proportionality between part load and efficiency, giving the lowest energy consumption for close to no load. This is not correct. The resulting deviation in production volume is found insignificant, but the higher efficiency for lower part loads does favor an over-dimensioning of the electrolysis component of the plant.

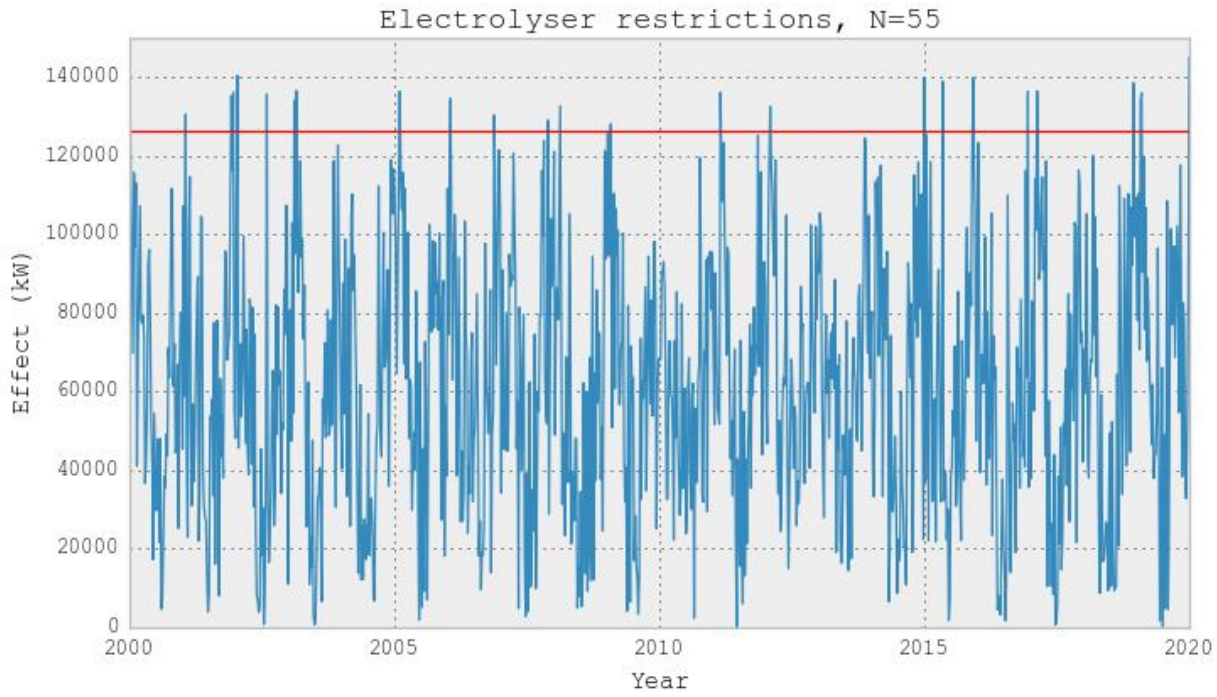

Figure 5.2: average weekly power input to the electrolysis plant (blue), and the optimal electrolysis capacity (red).

Voltage degradation over time is neglected. After 7 years of operation, the energy consumption may be about 10 % higher than in the beginning of the operation period. This results in a somewhat lower production volume in reality than simulated.

5.2.3 Liquefier

For the optimal plant dimensions found, a liquefaction capacity of 48.9 tons/day is required. However, the average production is 950 kg/h, corresponding to 22.8 tons/day. This constitutes about 47 % of maximum liquefaction capacity. The utilization of the liquefaction plant is thus low.

The simulation of the production of liquid hydrogen is performed in the time domain with an hourly resolution. The production is assumed completed at an instant, with no delays between the electrolysis and the liquefaction processes. This is inaccurate.

5.2.4 Storage

Boil-off losses, as assumed 0.06 % of total storage capacity per day (Amos 1998), constitute about 0.8 % of annual production volume of LH2. In comparison, does the amount LH2 dumped due to storage

restrictions constitute about 0.4 %. The total boil-off losses are assumed a constant ratio of total storage capacity, but may vary with the tank capacity, the number of tanks and storage filling level.

The average storage filling level at the time of delivery is 160 tons, which is about 53 % of the maximum capacity. How the storage is filled and emptied every week in the simulations is shown in **Figure 5.3** for the year 2005. The storage capacity is shown with red.

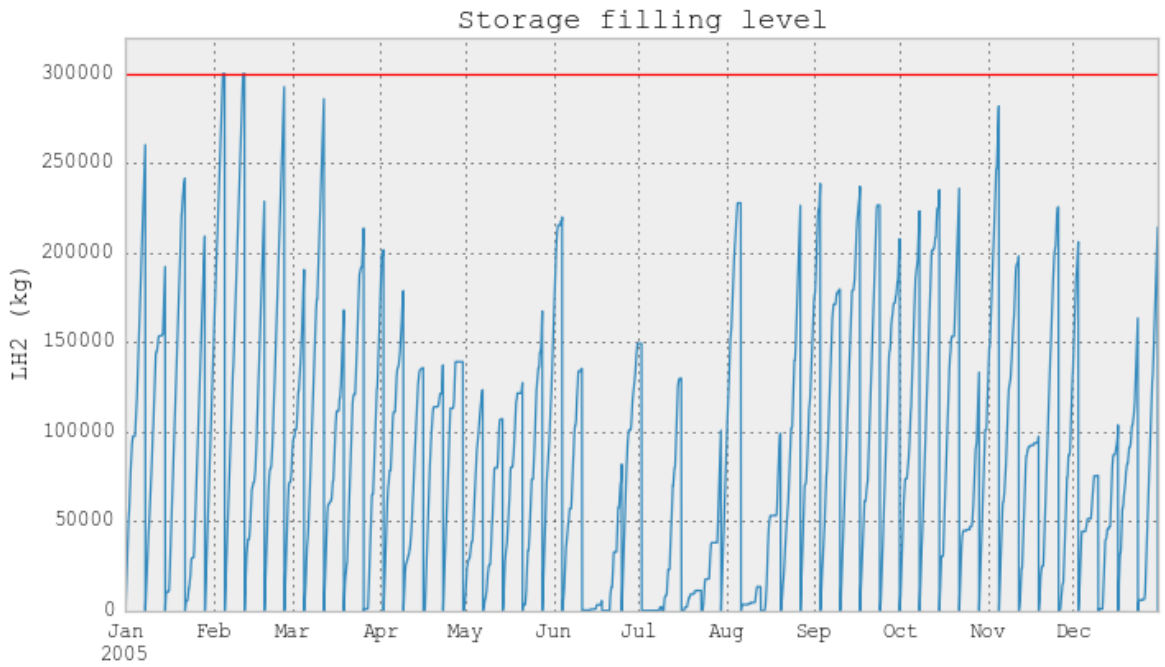

Figure 5.3: Storage filling level. Storage capacity shown in red.

5.2.5 Delivery

The average delivery volume of 160 tons gives an average utilization of the carrier ships of about 53 %.

5.3 Costs

The investment costs of wind power is somewhat conservative. Many components, like infrastructure and grid, already exist at Raggovidda and may be used during an expansion. In addition, one can benefit from the experiences from the construction of stage 1 of Raggovidda wind farm. Thus, the construction of stage two is expected to be cheaper per MW installed than normally applies for new wind farms, which is about 1.37 MEUR/MW. The O&M costs are assumed constant

over the entire lifetime of the plant. In reality, maintenance costs usually increase towards the end of the operation period, but this has been disregarded.

The investments costs of the electrolysers are varying linearly with capacity, and thereby giving no economies of scale. The regeneration costs are equally distributed over the lifetime of the plant and added to the O&M costs, giving a constant O&M of 6 % of the investment costs. In reality the regeneration appears as a reinvestment after 7 and 14 years of operation. The simplification by equally distributing the costs over the lifetime are therefore somewhat inaccurate.

Many sources of information were found on liquefier costs, most at a level of about 900 EUR/(kg/day) capacity. The economies of scale are large, and a sizing exponent of 0.57 was therefore chosen, as defined in equation (2.13). For the optimal plant dimensions found, a liquefaction capacity of 48.9 tons/day is required, giving an investment cost of 958 EUR/(kg/day).

Costs of storing liquid hydrogen were found to vary significantly between different sources. The value chosen is among the lower estimates, but due to the large economies of scale for storage facilities, considered applicable for the dimensions at Raggovidda. For the optimal storage capacity found, 300 t, the investment costs amounts to about 28 EUR/kg hydrogen storage capacity. The operation and maintenance costs of liquid hydrogen storage is set to a constant level of 2 % of the investment, an uncertain value, because few sources were found on this area.

The delivery cost is calculated based on distribution of LNG in Norway, due to lack of data for liquid hydrogen carriers. The cost per Nm^3 of LNG is converted to the equivalent cost per kg LH2, provided the same transport volume per ship. The cost is then doubled to account for a longer delivery distance and the higher expenses of new technology. The calculated cost of 0.79 EUR/kg LH2 is still considered a low estimate, and oversea delivery costs for liquid hydrogen may be much higher.

Based on the current weak global economic situation an interest rate of 5 % is considered applicable.

5.4 Future perspectives

According to the European Hydrogen Roadmap (Wurster and Ludwig-Bölkow-Systemtechnik 2008) the future target for hydrogen fuel cost is 4 EUR/kg in 2020 and 3 EUR/kg in 2030. This means that hydrogen production must be more cost efficient in the future.

The following sections give an overview of future perspectives and expected development of the hydrogen technology.

5.4.1 Electrolysis technology

The main challenges of alkaline electrolysis are the low current density, low operating pressures and limited modes of dynamic operation. However, technology improvements are expected due to increased deployment of electrolysers in the future energy system. It is expected that most commercial electrolysers will provide hydrogen at about 30 bars in 2030, reducing the cost of external compressors (Bertuccioli et al. 2014).

The cost of electrolysis technology is expected to decrease significantly over the next years, mainly due to increased production volumes and more cost-efficient production techniques. The system cost of alkaline electrolysers is expected to decrease from today's level of 1,000 – 1,500 EUR/kW to about 600 EUR/kW in 2020 (Bertuccioli et al. 2014).

Today PEMEC technology is only available at smaller scale than alkaline. However, many manufacturers are developing larger systems, and MW-scale stacks are expected from 2015 (Bertuccioli et al. 2014). On January 14th this year, Proton OnSite announced the commercial launch of a 1 and 2 MW PEM Hydrogen Generation System (Business Wire 2015). In Germany, Mainz Energy Park is under construction and is planned opened in July 2015 (Energiepark Mainz 2015). With a peak performance of up to 6 MW, the park will be the world's largest electrolysis facility using PEM technology.

Solid oxide electrolysers, which operate at high temperatures, may produce hydrogen with much lower electricity inputs than conventional electrolysers (Bertuccioli et al. 2014). Further development of the technology is however required to demonstrate and prove their potential.

5.4.2 Liquefaction technology

A liquefaction plant of the scale considered here has not been built so far. In Europe and Asia only a handful of liquefaction plants exist, with a capacity of up to 10.5 tons/day (Tzimas et al. 2003). In North-America there are 10 liquefaction plants, with capacities ranging from 6 to 35 tons/day (Drnevich 2003).

The IDEALHY, Integrated Design for Efficient Advanced Liquefaction of Hydrogen, is an EU-funded project completed in October 2013. Its target was to develop an economic and high-effective liquefaction technology for hydrogen in Europe and thereby stimulate investments in infrastructure and refuelling stations for hydrogen. By developing a new process design for LH2 production capacity of up to 200 tons per day, it aimed at reducing the specific energy consumption by 50 %, i.e. to a

level of about 6 kWh/kg. The developed technology remains to be demonstrated, and a large-scale plant for this purpose is under planning.

Such a large reduction in energy consumption reduces the specific production costs significantly. However, the improved technology have higher investment costs. An investment of 105 million Euro is assumed for a plant of 50 tons/day, giving a specific cost of 2100 EUR/(kg/day) (Stolzenburg and Mubbala 2013). This is more than the double of the assumed cost in this thesis.

5.4.3 Liquid hydrogen carrier ships

LH2 ships are under development, but have not been built so far. Kawasaki's prototype carrier ship developed have a capacity of 2,500 m^3 enabling distribution of up to 177 tons of liquid hydrogen. The construction of the ship is planned in the period 2014 – 2017, aiming at an operation startup in 2017. At the initial stage the ships will be powered by diesel engines, but Kawasaki aims at developing a system where the boil-off hydrogen gas can be used for propulsion of the ships.

In the longer term, a larger version of the liquid hydrogen carrier using spherical containment vessels has been proposed. With a total capacity of 250,000 m^3 the ship can deliver up to 17,700 tons of hydrogen.

6 Summary & Conclusions

Raggovidda wind farm is assumed expanded from 45 MW to 200 MW, and hydrogen is assumed produced from excess wind power. The grid restriction is set to 50 MW, and whenever the wind power exceeds 50 MW, hydrogen is produced.

Based on a Weather Research and Forecast model run by Kjeller Vindteknikk, as well as wind- and production data from Raggovidda wind farm, a time-series of power of 20 years with an hourly resolution is developed. With this as an input, hydrogen production is simulated with the use of Python. Alkaline atmospheric electrolysers of 2.3 MW are considered. Liquid storage and delivery is considered the best solution for the large dimensions at Raggovidda. Storage is assumed emptied once a week by two carrier ships operating in shuttle with a delivery range of 2,000 – 2,500 nautic miles. Electrolyser and storage capacity are design variables. The liquefaction capacity follows from the electrolysis maximum output, and the ship size required follows from the storage capacity.

By minimizing production costs, the optimal dimensions of the plant are found. Provided a 5 % result cost interval, the optimal electrolysis capacity ranges from 103.5 – 151.8 MW and the optimal weekly storage ranges from 300 – 400 tons of hydrogen. This requires a liquefaction capacity of 49 – 58 tons/day, and a carrier ship size of 4,240 – 5,650 m^3. The production cost is calculated to 4.23 – 4.34 EUR/kg. With a charge of about 10 EUR/kg hydrogen at refuelling stations, a revenue of more than 5 EUR/kg may be achievable.

References:

Agency for Natural Resources and Energy (2014), 'Summary of the Strategic Road Map for Hydrogen and Fuel Cells', in Trade and Industry Ministry of Economy (ed.), (Ministry of Economy, Trade and Industry).

Akershus County Council (2014), 'Hydrogenstrategi 2014-2025', (Oslo).

Amos, Wade A (1998), *Costs of storing and transporting hydrogen* (National Renewable Energy Laboratory Golden, CO, USA).

Bertuccioli, Luca, et al. (2014), 'Study on development of water electrolysis in the EU', (Final Report edn.: FCH JU).

Boundy, Bob, et al. (2011), *Biomass Energy Data Book: edition 4*, ed. Oak Ridge National Laboratory (4 edn.: U.S. Department of Energy).

Business Wire (2015), 'Proton OnSite Introduces World's First PEM Megawatt Electrolyzer for the Growing Global Energy Storage Market', in Kathleen Mullins (ed.), (Wallingford; Wallingford: Business Wire,).

Byrkjedal, Øyvind, Åkervik, Espen, and Kjeller Vindteknikk (2009), 'Kartbok 1a: Årsmiddelvind i 80m høyde', *Vindkart for Norge* (Oslo: NVE), 43.

Dalløkken, Per Erlien (2014), 'På 12 år har Toyota senket kostnader på brenselcellebiler med 95 prosent', *Teknisk Ukeblad*.

David, Mike, et al. (2002), 'National Hydrogen Energy Roadmap', in United States Department of Energy (ed.), (Washington, DC: United States Department of Energy).

DnB Markets (2015), 'Gjennomsnitsskurser 2015', *Historiske valutakurser* <https://translate.google.com/#no/en/valutakurs>, accessed April 2.

Drnevich, Raymond (2003), 'Hydrogen Delivery, Liquefaction and Compression', in Praxair (ed.), *Hydrogen Delivery Workshop* (Tonawanda, NY: U.S Department of Energy).

Einang, Per Magne, et al. (2005), 'Framtidsbilde for norsk naturgassdistribusjon, 2015-2025', (MARINTEK, SINTEF), 86.

Energiepark Mainz (2015), 'Energipark Mainz: Erstes elektrolysesystem eingetroffen', in Michael Theurer (ed.), *Spezialkran liefert wichtige Anlagenteile - Eröffnung Anfang Juli geplant* (Mainz; Mainz: Energipark Mainz,).

Essler, Jürgen, et al. (2012), 'Report on Technology Overview and Barriers to Energy- and Cost-Efficient Large Scale Hydrogen Liquefaction', (IdealHy).

Gerboni, R. and Salvador, E. (2009), 'Hydrogen transportation systems: Elements of risk analysis', *Energy,* 34 (12), 2223-29.

Greiner, Christopher Johan (2010), 'Sizing and operation of wind-hydrogen energy systems'.

Hydrogen Delivery Technical Team (2013), 'Hydrogen Delivery Technical Team Roadmap', (U.S. Drive Partnership).

IDEALHY (2012), 'Design Principles for High-Efficiency Hydrogen Liquefaction Processes', *World Hydrogen Energy Conference* (Toronto, Canada).

IHS (2015), 'Hydrogen', *Chemical Economics Handbook* (updated August 1) <https://www.ihs.com/products/hydrogen-chemical-economics-handbook.html>, accessed April 15.

Kawasaki (2014), 'Kawasaki Heavy Industries Obtains AiP for Liquefied Hydrogen Carrier Cargo Containment System', (web: Kawasaki Heavy Industries Ltd.).

Korneliussen, Øivind (2015), 'Personal communication', in Lotte Løland (ed.).

Korpås, Magnus (2004), 'Distributed Energy Systems with Wind Power and Energy Storage', (Doktoravhandlinger ved NTNU: Fakultet for informasjonsteknologi, matematikk og elektroteknikk).

Laguna, M. A. (2012), 'Recent advances in high temperature electrolysis using Solid Oxide Fuel Cells: A review'.

Larminie, James and Dicks, Andrew (2009a), 'Fuelling Fuel Cells', *Fuel Cell Systems Explained* (John Wiley & Sons, Ltd,.), 229-308.

--- (2009d), 'Operational Fuel Cell Voltages', *Fuel Cell Systems Explained* (John Wiley & Sons, Ltd,.), 45-66.
Lie, Øyvind (2013), 'Vil transportere overskuddskraft som hydrogen', *Teknisk Ukeblad*.
Linde AG 'LH2 - Tank System', (Web: Linde AG).
Meterologisk institutt *eKlima*. in eKlima online database], Meterologisk institutt, (February 13).
Mueller-Langer, F., et al. (2007), 'Techno-economic assessment of hydrogen production processes for the hydrogen economy for the short and medium term', *International Journal of Hydrogen Energy,* 32 (16), 3797-810.
Nationen (2015), 'Kollektivtrafikken skal bli helgrønn innen 2025', *Nationen,* January 29.
NEL Hydrogen 'Efficient electrolysers for hydrogen production', (web: NEL Hydrogen).
Nord Pool Spot (2015), *Elspot prices Tromsø, Norway*. Nord Pool Spot (March 2).
NORWEA (2012) *Vindkraftens ABC* [online text], NORWEA <http://www.norwea.no/bibliotek.aspx>
NORWEA and Energi Norge (2015), 'Vindinfo', <http://www.vindinfo.no/>, accessed March 20th.
NVE (2015), 'Elsertifikater: Kvartalsrapport nr. 4 2014', in NVE (ed.), *Kvartalsrapporter* (web: NVE).
PATH (2011), 'Annual Report on World Progress in Hydrogen', in Partnership for Advancing the Transition to Hydrogen Association (ed.), (Washington D.C), 70.
Ramachandran, Ram and Menon, Raghu K. (1998), 'An overview of the industrial uses of hydrogen', *International Journal of Hydrogen Energy,* 23 (7), 593-98.
Riis, Trygve, et al. (2006), 'Hydrogen Production R&D: Priorities and Gaps', in IEA Hydrogen Co-Ordniation Group (ed.), *R&D Priorities and Gaps* (OECD/IEA).
Siemens AG (2014), 'Siemens D3 platform - 3.0-MW and 3.2-MW direct drive wind turbines', in Siemens AG (ed.), (web: Siemens AG).
Simonsen, Bjørn (2015a), 'Hydrogen i Norge frem mot 2040', in Bjørn Simonsen (ed.), *Den norske gasskonferansen* (Oslo: Den norske gasskonferansen), 29.
--- (2015d), 'Personal communication', in Lotte Løland (ed.).
Springer (2014), 'Power-to-gas technology and business models'.
Statistisk Sentralbyrå (2013) *Statistisk årbok 2013* [online text], Statistisk Sentralbyrå <http://www.ssb.no/befolkning/artikler-og-publikasjoner/_attachment/140702?_ts=1415a7ca078>
Statnett SF (2013), 'Grid Development Plan 2013', (Statnett SF), 114.
Stolzenburg, K. (2014), 'Large Wind-Hydrogen Plants in Germany: The Potential for Success', in K. Stolzenburg (ed.), *Joint NOW GmbH – FCH JU Water Electrolysis Day* (Brussels: FCH JU).
Stolzenburg, K. and Mubbala, R. (2013), 'Hydrogen Liquefaction Report', *Integrated Design for Demonstration of Efficient Liquefaction of Hydrogen (IDEALHY)* (Web: Fuel Cells and Hydrogen Joint Undertaking (FCH JU)).
Teknisk Ukeblad (2015), 'Raggovidda vindpark', (www.tu.no: Teknisk Ukeblad,).
Toyota Motor Sales (2015), 'The Tyota FCV - A turning point from the indisde out', *The turning point* <http://www.toyota.com/fuelcell/fcv.html>, accessed April 15.
Tzimas, Evangelos, et al. (2003), 'Hydrogen Storage: State-of-the-Art and Future Perspective', (Luxembourg: European Commission).
Varanger KraftNett AS (2013), 'Lokal Energiutredning, Berlevåg kommune 2013', in Varanger KraftNett AS (ed.), (Berlevåg municipal), 28.
Wurster, Reinhold and Ludwig-Bölkow-Systemtechnik (2008), 'The European Hydrogen Energy Roadmap'.
Yang, Christopher and Ogden, Joan (2007), 'Determining the lowest-cost hydrogen delivery mode', *International Journal of Hydrogen Energy,* 32 (2), 268-86.

Appendix A: Further analyses

For the optimal plant dimensions found in the thesis, i.e. an electrolysis capacity of 126.5 MW and a storage of 300 tons, further analyses have been made. The following section highlights the main analyses.

Week of most production

The week of most production is depicted in **Figure A-1**. During seven days more than 330 tons of liquid hydrogen is produced.

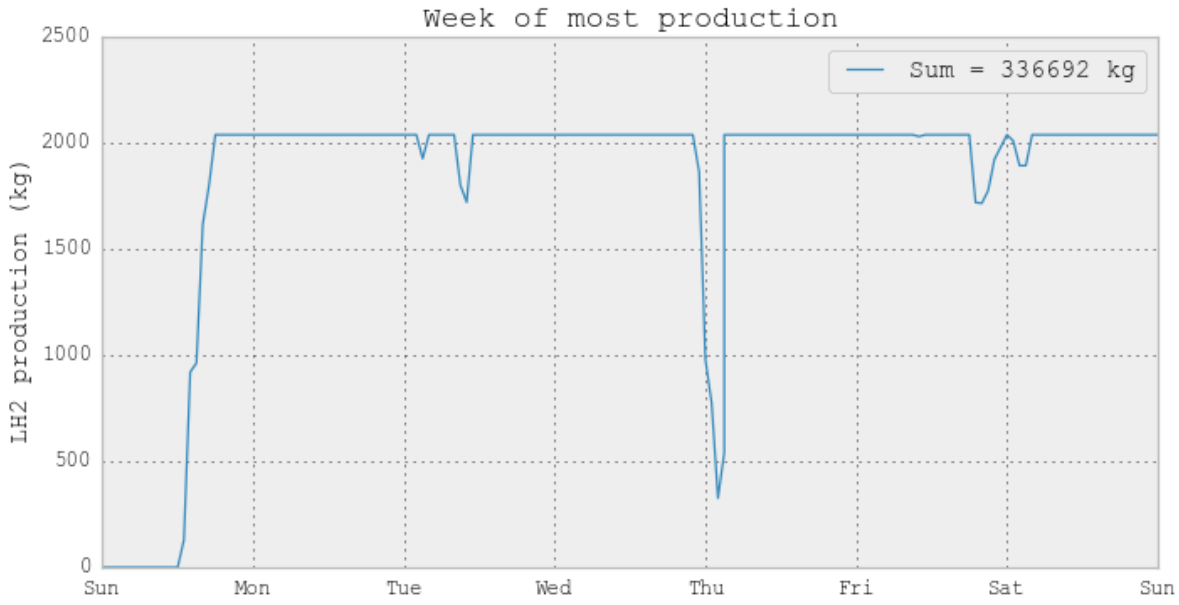

Figure A-1: week of most production.

During the best week of the entire 20-year lifetime as much as 337 tons of LH2 is produced. This corresponds to 7 days of almost maximum operation of the electrolysers, which would give a production of 434 tons. The utilization rate of the electrolysers during the best week is thus 77.6 %.

Week of least production

The week of least production is depicted in **Figure A-2**. In seven days only a total of 58 kg of hydrogen is produced.

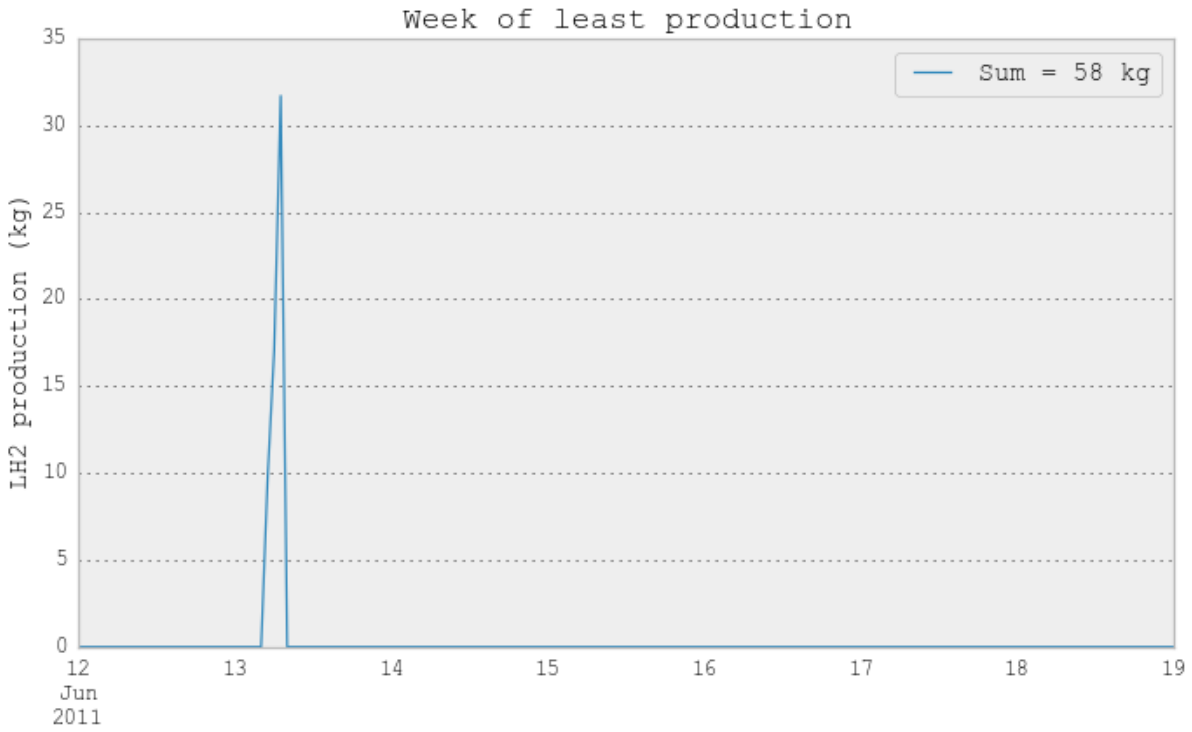

Figure A-2: week of least production.

During the week of least production only 58.5 kg of LH2 is produced. This corresponds to a week of low wind speeds, which means that the electricity output from the wind farm barely exceeds 50 MW. Almost all of the wind power produced is distributed on the electricity grid.

Average production per month

The average production volume per month is shown in **Figure A-3**, with values ranging from 374 tons in June to 890 tons in January.

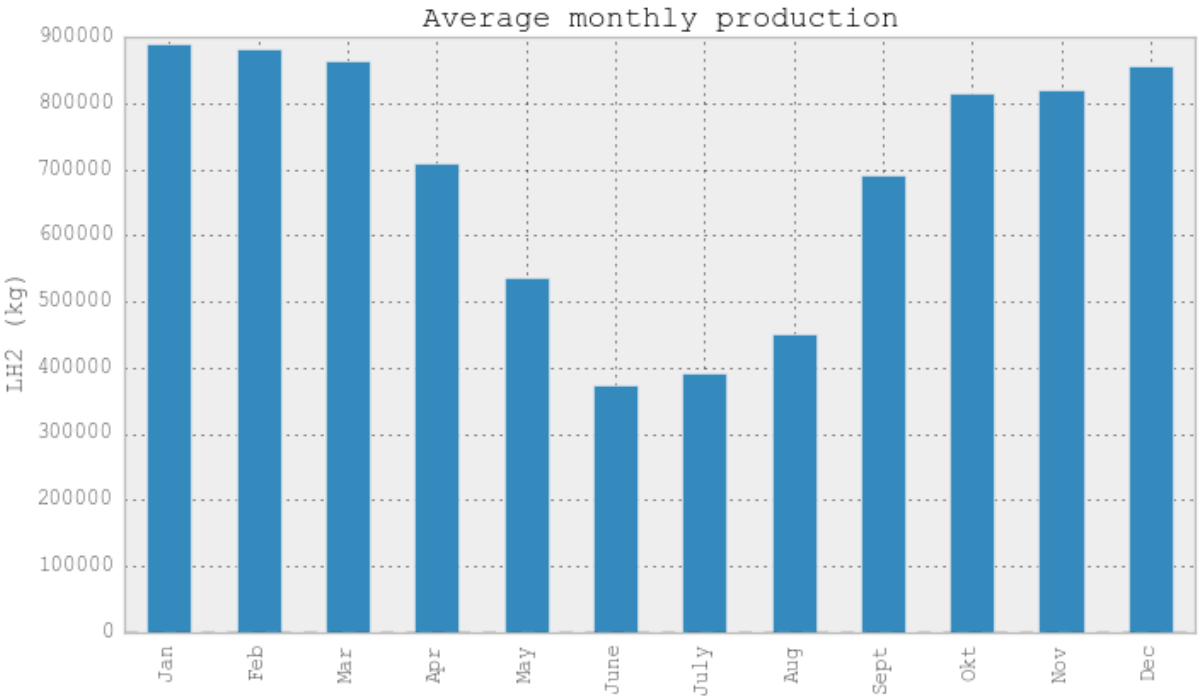

Figure A-3: average hydrogen production volume per month.

The production of hydrogen is higher in the winter months than during the summer. In fact, the average production in May-August only constitutes about 21 % of the average annual production volume. On the other hand, do the four best months, December to March, constitute about 42 % of average annual production. These variations over the year can be explained by the much higher wind speeds in the winter months than in the summer. According to the wind series, the average wind speed in January is of 9.9 m/s while the average wind speed of June is of 6.2 m/s. This variation corresponds to a big difference in wind power output, as according to the power curve for the wind farm, ranges from about 14 MW to about 35 MW.

Annual variations

The annual production volume of liquid hydrogen is shown in **Figure A-4**. The average volume is 8234 tons. The values ranges from 7525 tons to 9122 tons, which is about ± 12 % of average. This shows that the annual production is relatively stable over the lifetime of the plant.

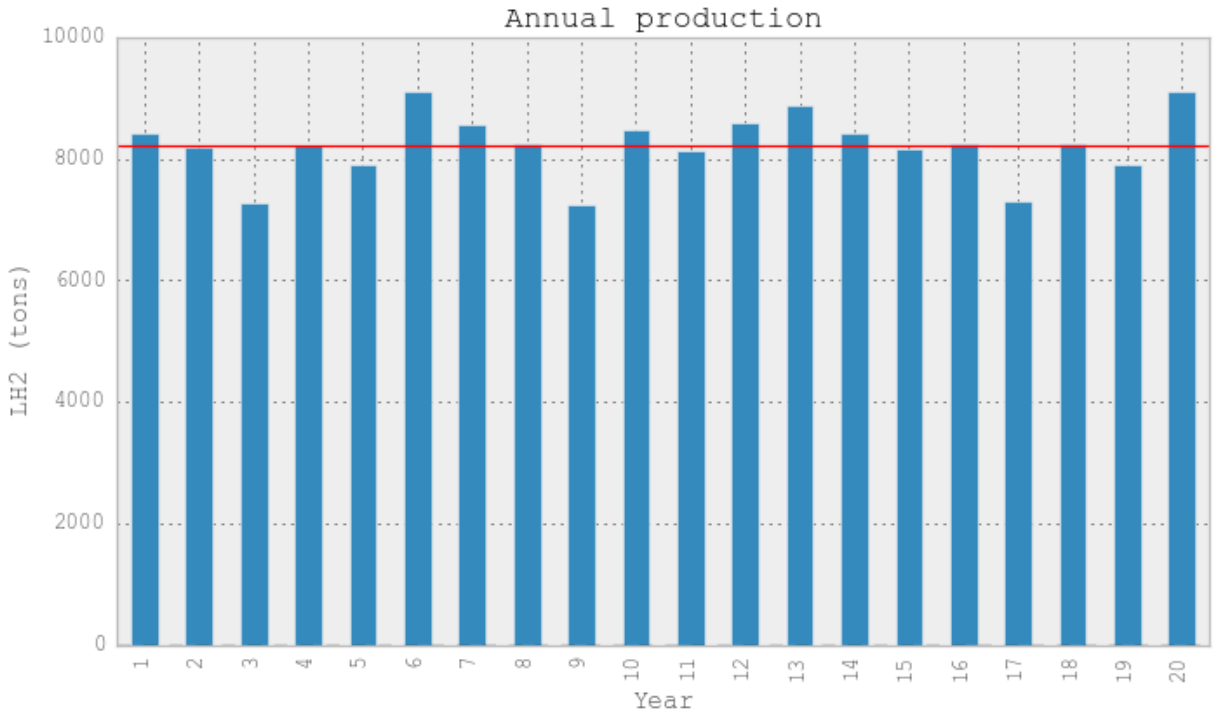

Figure A-4: annual hydrogen production.

Sensitivities

Compared to today's electricity distribution, an expansion of Raggovidda wind farm from 45 MW to a capacity of 200 MW will cause increased sales of electricity. This do not directly influence the hydrogen production cost, but do make the investment in the wind farm expansion more profitable. To account for the extra income, the annual extra income from electricity sales from wind power below 50 MW is thus subtracted from the annual capital costs. Thus, the annual wind costs consist of investment costs, O&M costs and electricity sales.

The base case used in the simulations is calculated based on an electricity price of 40 EUR/MW, which is the average price of the last 12 years in Finnmark. **Figure A-5** shows how the production cost of hydrogen may vary with different electricity prices. The elcertificate price is assumed to be 19 EUR/MWh.

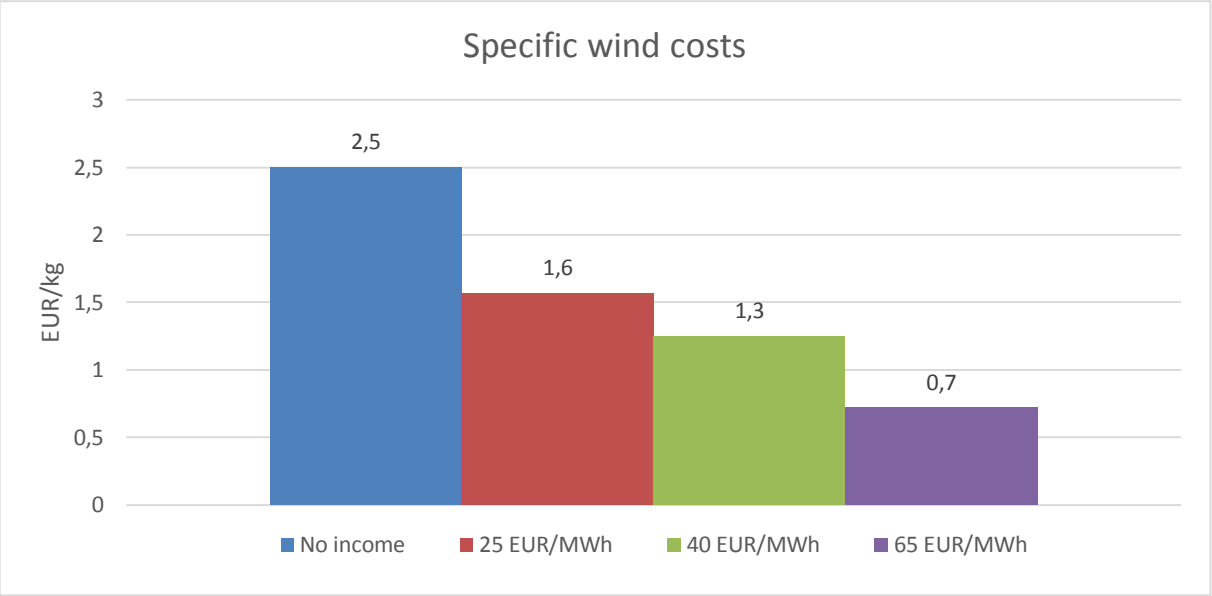

Figure A-5: annual wind costs per kg hydrogen produced, adjusted for different electricity prices. A base case of 40 EUR/MWh is used in the thesis.

Without crediting the extra income from sales of electricity compared to today's electricity distribution to the expansion of the wind farm, the annual wind costs amount to 2.5 EUR/kg hydrogen delivered. The base case gives a cost of 1.25 EUR/kg. If the electricity price in the future is low, about 25 EUR/MWh, the cost increases to 1.57 EUR/kg, but if the price increases to a level of 65 EUR/MWh, the cost may decrease to only 0.72 EUR/kg.

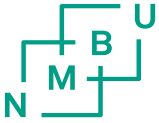

Norwegian University
of Life Sciences

Postboks 5003
NO-1432 Ås, Norway
+47 67 23 00 00
www.nmbu.no